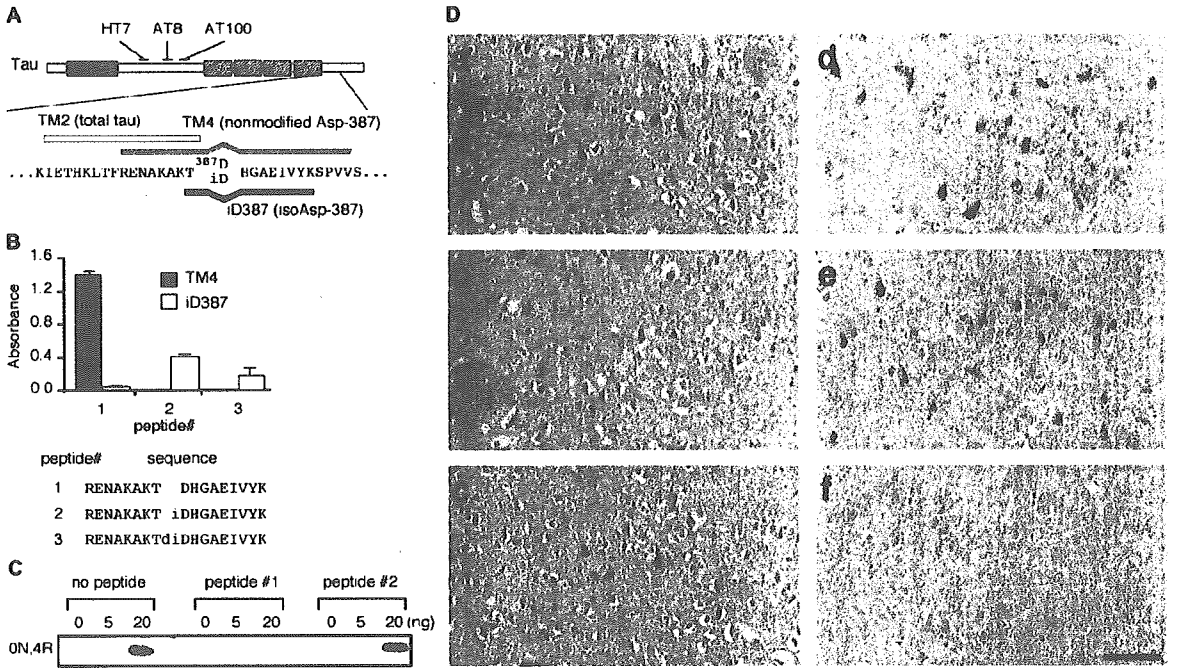

FIGURE 2. Characterization of TM4 and iD387. **(A)** The antibodies used in this study and the locations of their epitopes along the longest, 441-residue human tau molecule (dark gray boxes, aminoterminal inserts; striped boxes, microtubule-binding domains). The gray and black bars indicate the immunogens for TM4 and iD387, respectively. ID, isoAsp-387. **(B)** Specificities of TM4 and iD387 toward isomerized and unmodified synthetic peptides as assessed by one-site enzyme-linked immunosorbent assay. A plate coated with 2.5 μg of either peptide (residues 379–395 of tau; lower panel) was incubated with either TM4 or iD387. TM4 reacted only with unmodified peptide (peptide 1). iD387 strongly labeled isoAsp-peptide (2), but scarcely Asp-peptide (1). Dextro-isoAsp (diD) peptide (3) was partially labeled with iD387, but not with TM4. Bars indicate means ± standard error of 3 independent experiments. **(C)** Indicated amounts of recombinant 0N4R tau were subjected to Western blotting using TM4 or TM4 preabsorbed with Asp- or isoAsp-peptide. The TM4 immunoreactivity is markedly reduced by preabsorption with Asp-peptide (1) but not with isoAsp-peptide (2). **(D)** To test the specificity at the immunocytochemical level, AD sections were probed with TM4 **(a–c)** and iD387 **(d–f)** preabsorbed without **(a, d)** or with Asp-peptide (1, **[b, e]**) and isoAsp-peptide (2, **[c, f]**). TM4 or iD387 staining was completely abolished by preabsorption with Asp-peptide (1, **[b]**) or isoAsp-peptide (2, **[f]**), respectively. Scale bar = 50 μm.

never found in the corresponding fractions from control brains (Fig. 3A).

TS-soluble tau in control and AD brains was labeled with TM4 but never with iD387 (data not shown). TM4 preferentially labeled PHF-tau in the Sarkosyl-insoluble, SDS-soluble fraction, but only faintly labeled PHF smear (Fig. 3E). In contrast, iD387 intensely labeled PHF smear in SDS-soluble and SDS-insoluble fractions (Fig. 3F). This is consistent with the view that PHF become progressively insoluble and that PHF-tau is gradually converted to PHF smear in vivo (21). Thus, it is reasonable to postulate that TM4-labeled tau represents the more recent tau deposition and iD387-labeled tau represents an earlier deposition.

Tau Inclusions Labeled With Asp-387- and isoAsp-387-Specific Antibodies

NFTs, NTs, and dystrophic neurites (DNs; senile plaque-associated neurites) were examined for the extent of TM4 and iD387 immunoreactivities compared with TM2 immunoreactivity. TM2 was assumed to label all intra- and extracellular NFTs, because its epitope is located in the "PHF core" (Fig. 4A, E) (10). In contrast, AT8 failed to label extracellular NFTs, because the epitope is lost in those tangles, possibly as a result of proteolytic processing (Fig. 3).

We have focused on the hippocampus, the most vulnerable area in AD, which contains all types of NFTs—pre-tangles, intracellular, and extracellular, tangles—in varying proportions (5, 38). In Braak stages III/IV, TM2 intensely labeled NFTs and NTs in the CA1 region. The densely packed flame-shaped NFTs surrounding the nucleus are representative of intracellular NFTs. In adjacent sections, these NFTs were labeled with both TM4 and iD387 (Fig. 4A–D). NTs were well labeled, but more intensely with iD387. DNs were labeled to the same extent with both antibodies. In the hippocampus at Braak stages V/VI, TM2 labeled innumerable NFTs (Fig. 4E). These were mostly extracellular NFTs, because of their flattened configuration and the absence of nuclei. These NFTs, except for a few, were hardly labeled with TM4 (Fig. 4F). This suggests that extracellular NFTs are mainly composed of tau containing modified Asp-387. However, unexpectedly, only a small fraction of the extracellular NFTs was labeled strongly with iD387, whereas the remainder was only faintly stained (Fig. 4G). NTs in the brains at Braak stages V/VI were also scarcely labeled with TM4 or iD387 (data not shown).

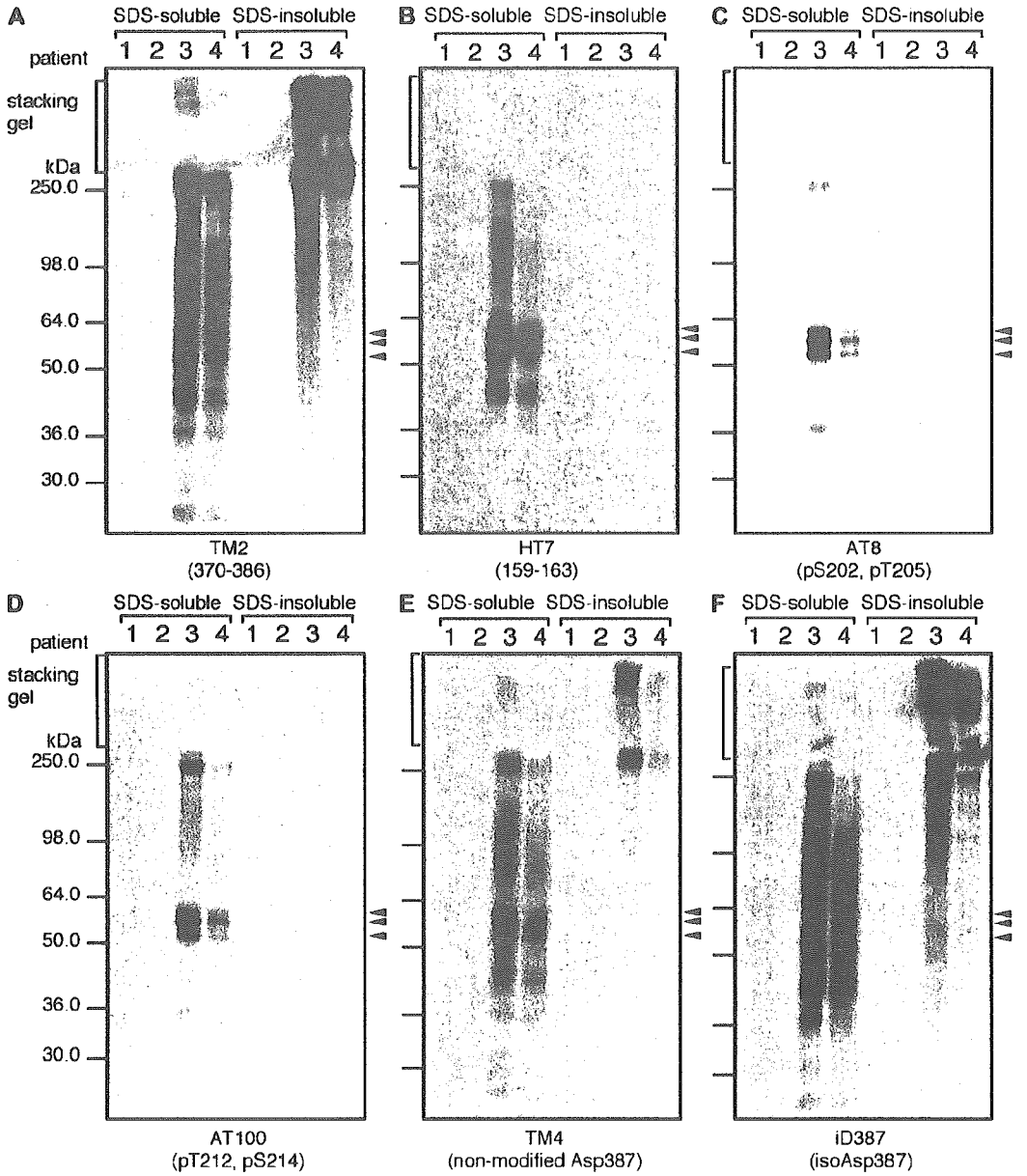

FIGURE 3. Full-length PHF-tau and PHF smear as labeled with TM4 or iD387. Sarkosyl-insoluble pellets from control (lanes 1 and 2) and AD (lanes 3 and 4) brains were further fractionated by solubility in 1% SDS. Each fractionated sample was subjected to Western blotting using the indicated antibodies. TM2, a pan-tau antibody, labeled characteristic triplet bands composing PHF-tau (arrowheads) and PHF smear **(A)**. In sharp contrast, HT7 **(B)**, AT8 **(C)**, and AT100 **(D)**, intensely labeled PHF-tau but not PHF smear, indicating loss of the aminoterminal and midportions in PHF smear. The same fractions were also subjected to Western blotting with TM4 **(E)** and iD387 **(F)**. Although the epitopes of TM4 and TM2 are located very closely (see Fig. 2), TM4 intensely labeled PHF-tau, but only weakly PHF smear in the SDS-soluble fraction and barely PHF smear in the SDS-insoluble fraction. In contrast, iD387 intensely labeled PHF smear in both SDS-soluble and insoluble fractions, which overshadowed PHF-tau.

TM2-positive and TM4-positive NFTs were quantified in the CA1 region. Because the isomerization of Asp is a spontaneous chemical reaction, the rate of isoAsp formation in PHFs can be regarded as not so variable. Thus, TM4-positive NFT counts reflect the generation rate of NFT-bearing neurons at the time of death. Along with the total numbers of NFT, mild (0–50/3.2 mm^2), moderate (51–100/3.2 mm^2), advanced (101–150/3.2 mm^2), and severe (over 151/3.2 mm^2), those of TM4-positive NFT increased from mild to moderate cases, but rather leveled off in moderate to severe cases (Fig. 5). Statistically

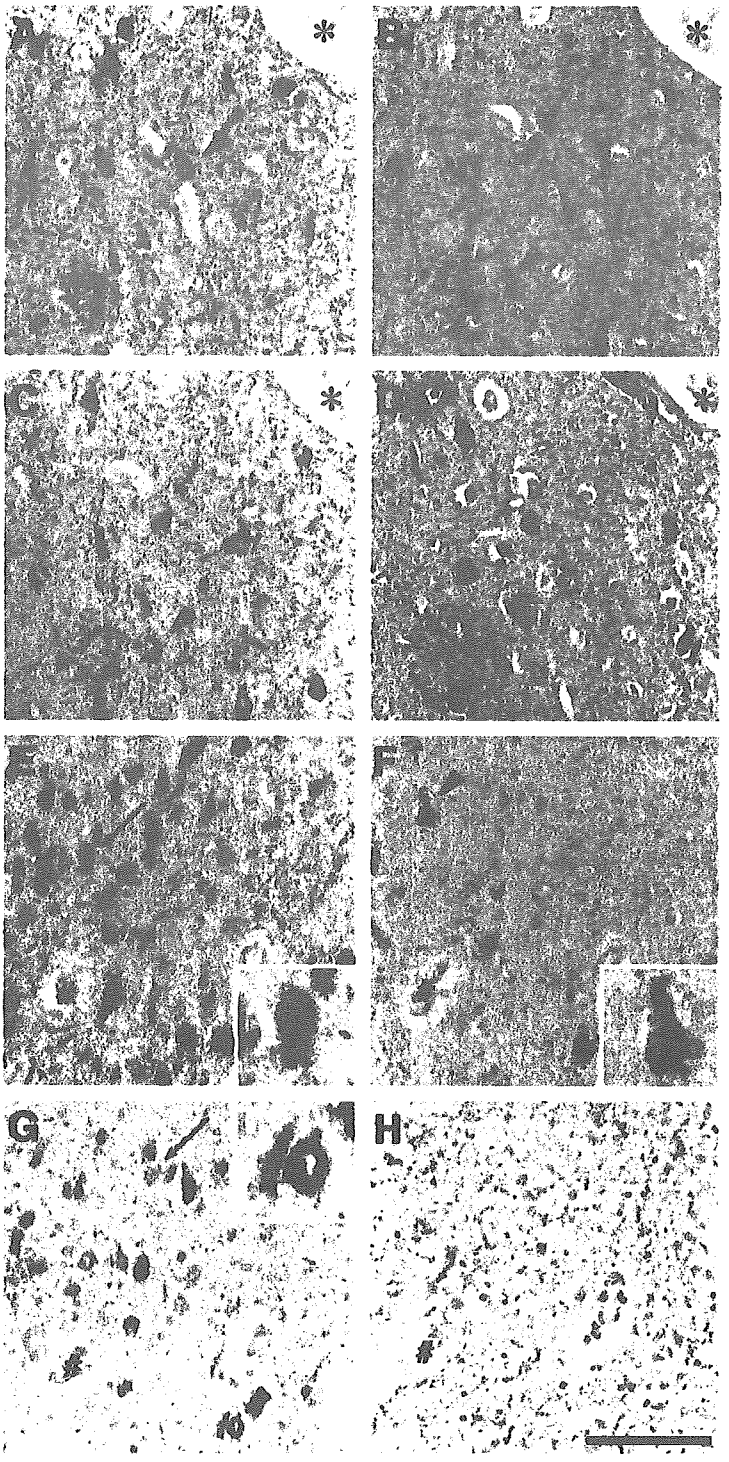

FIGURE 4. Immunocytochemistry using TM4 and iD387. Paraffin-embedded sections from the hippocampus at Braak stages III/IV **(A–D)** and Braak stage V/VI **(E–H)** were immunostained with TM2 **(A, E)**, TM4 **(B, F)**, iD387 **(C, G)**, and AT8 **(D, H)**. Note that all antibodies intensely stained intracellular neurofibrillary tangles (NFTs) (arrowheads and inset) and neuropil threads in the hippocampus at the early neocortical stage **(A–D)**. In contrast, extracellular NFTs (arrows and inset) were hardly stained with TM4 **(F)** or iD387 **(G)** and were not stained with AT8 **(H)**. *, # indicate the same vessels in adjacent sections. Scale bar = 100 μm.

significant differences in the TM4-positive NFT counts were observed only between mild and moderate cases (Fig. 5). Thus, TM4-positive NFT appeared to be constant even though the total NFT number increased from moderate to severe cases. This unexpected finding raises the possibility that NFTs are produced at a constant rate irrespective of the disease stage and are also constantly converted to TM4-negative (extracellular) NFTs in the hippocampus.

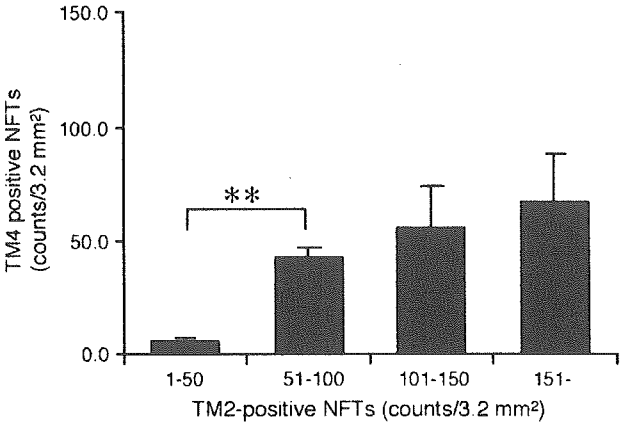

FIGURE 5. Semiquantification of TM2- and TM4-positive neurofibrillary tangles (NFTs) in the hippocampus. TM2- and TM4-positive NFTs per 3.2 mm^2 in the hippocampi of 53 non-Alzheimer disease (control) subjects and patients with Alzheimer disease were counted. The numbers of TM4-positive NFTs are shown against the abundance of TM2-positive NFTs: mild (0–50, n = 23), moderate (51–100, n = 14), advanced (101–150, n = 6), and severe (>151, n = 9). The numbers of TM4-positive NFTs significantly increased from mild to moderate cases, but not so from moderate to severe cases. Means ± standard error. Statistically evaluated by 2-way analysis of variance, followed by Bonferroni/Dunn post hoc test. Asterisks indicate a statistically significant difference (**, $p < 0.01$).

Distinct Localization of Isomerized and Unmodified tau

To investigate the localization of Asp-387 and isoAsp-387 in NFTs and NTs, vibratome sections from the hippocampus or temporal cortex at Braak stage IV or above were double-stained with TM4 and iD387 and viewed under a confocal laser-scanning microscope. The specimens from 8 of 15 subjects were labeled with both antibodies, the remainder being labeled only with iD387. Storage of the specimens seemed to have a remarkable effect on the extent of TM4 and iD387 staining. Vibratome sections stored in sucrose at –20°C were not stainable with TM4, whereas iD387 staining was retained. This was not the case with paraffin-embedded sections or immediately frozen blocks. It is likely therefore that isoAsp formation through succinimidyl intermediates proceeds in the aqueous environment, irrespective of prior formalin fixation.

In the specimens from the 8 subjects, NFTs were labeled with both antibodies, whereas NTs were labeled predominantly with iD387. In 6 cases, NTs were labeled to a similar extent with these 2 antibodies. Double immunostaining clearly showed that the portions labeled with the 2 antibodies were distinct from each other. TM4 stained NFTs in proximal dendrites and neuronal perikarya, whereas iD387 stained NFTs up to more distal dendrites (Fig. 6A, B). The intensities of TM4 and iD387 staining varied even within a thread (Fig. 6C). Most commonly, TM4 intensely labeled the outer portion of a thread, and iD387 preferentially labeled its core portion (Fig. 6D, E). In the case of isoAsp-387-rich NTs, patchy and discrete TM4 staining on the surface of a thread was often evident (Fig. 6D). In general, DNs were better stained with TM4, and NTs were better stained with iD387 (Fig. 6F).

Isomerization of tau in P301L and R406W Brains

More than 30 exonic and intronic mutations have been identified in the tau gene in patients affected by frontotemporal dementia and parkinsonism linked to chromosome 17 (FTDP-17), which is characterized pathologically by extensive neuronal loss and formation of filaments composed of tau (39, 40). Among FTDP-17 mutations, the P301L mutation is well known for its aggressive clinical phenotype and the R406W mutation for its more slowly progressive phenotype (41). It is possible that some differences between P301L and R406W mutations, including the type of tau deposited (4R tau vs. 3R + 4R tau), distribution of the tau pathology (widespread vs. rather restricted), and the differences in the cell type affected (neuronal and glial cells vs. neuronal cells), may be related to the difference in the phenotype. To determine whether isomerization of the deposited tau occurs similarly in these brains, Sarkosyl-insoluble fractions from affected frontal cortices were prepared and subjected to Western blotting using TM2, TM4, and iD387. TM2 intensely labeled the PHF smear in the Sarkosyl-insoluble fraction from a R406W brain. In contrast, only 2 major bands at 64 and 68 kDa were labeled in P301L brains (Fig. 7). These results are consistent with previous reports (23, 33, 34). TM4 labeled 3 bands of PHF-tau in AD and R406W brains, and 2 major bands in P301L brains, but only faintly PHF smear. In contrast, iD387 labeled exclusively PHF smear in AD and R406W brains but none in P301L brains (Fig. 7). Thus, the Sarkosyl-insoluble tau from R406W brains is isomerized at Asp-387 to a much greater extent than in P301L brains. Immunocytochemical staining of P301L and R406W brains with these antibodies was also examined. In a P301L case, TM2 and TM4 stained innumerable pretangles in the frontal cortex, but iD387 did only faintly (data not shown). In contrast, NFTs in R406W brain were intensely stained with both antibodies. This is consistent with the Western blot data shown in Figure 7.

DISCUSSION

Differential visualization of Asp- (unmodified) and isoAsp- (modified) tau should provide us with a time window for the formation and evolution of tau inclusions in the human brain. As shown here, there is a much larger amount of isoAsp-387 in PHF smear than in PHF-tau. Thus, TM4 and iD387 make it possible to visualize recent and earlier deposited tau proteins, respectively. Although the rate of isoAsp formation in PHFs in vivo is unknown, an in vitro incubation study showed that isoAsp-387 tau is gradually generated and discrete tau bands are converted to a smear over months (23). Thus, it is reasonable to assume that the formation of PHF smear takes months, but not longer than years.

TM4 intensely immunostained intracellular NFTs, but hardly stained the most evolved extracellular NFTs. According

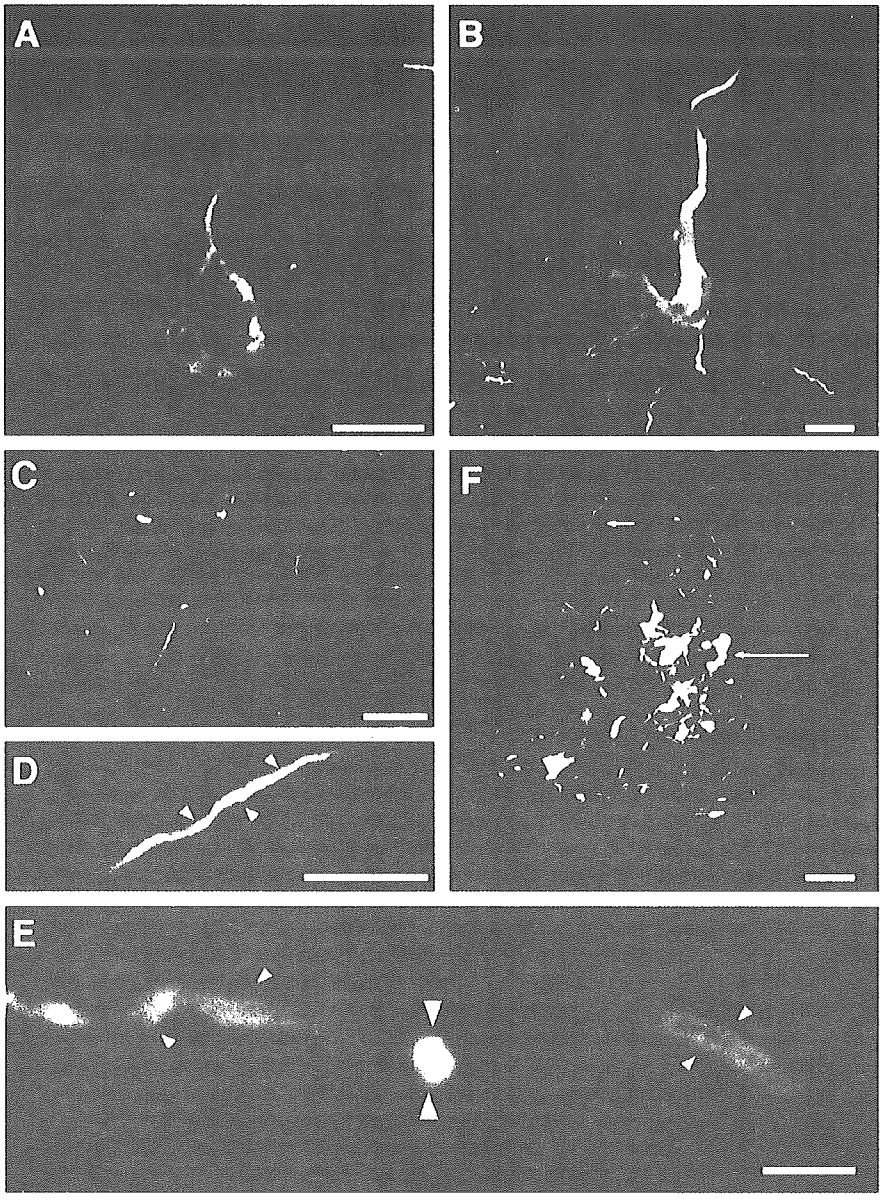

FIGURE 6. Differential distribution of TM4- and iD387-positive tau in neurofibrillary tangle (NFT), neuropil thread (NT), and dystrophic neurite (DN). Vibratome sections from Alzheimer disease temporal cortices or hippocampi were labeled with TM4 (green) and iD387 (red), and observed under a confocal microscope. Merged images in the temporal cortices of patient 1 **(A, F)** and patient 2 **(B)**, and in the hippocampus of patient 3 **(C)** are shown. TM4 preferentially labeled the NFTs in the proximal portion of dendrites and cell bodies, whereas iD387 labeled whole profiles of NFTs up to the distal potion of dendrites **(A, B)**. TM4 and iD387 immunoreactivities of NTs varied substantially **(C)**. When TM4 immunoreactivity is noticeable on NT, it is mostly located on its outer portion **([D, E]**, small arrowheads). A transverse section clearly shows that TM4 labeled the outer portion of a thread **([E]**, large arrowhead), whereas iD387 labeled the core portion. TM4 stained DNs (long arrow) to a greater extent than scattered NTs in the surrounding area (short arrow) **(F)**. Scale bars = **(A–D, F)** 10 μm; **(E)** 2 μm.

to recent studies, NFT-bearing neurons can live decades (42) and the maturation of NFT takes several years (43). Together with our results shown in Figure 4, the presence of unmodified tau, even in the terminal stages of NFTs, suggests that de novo synthesis of tau (and possibly other proteins) is still maintained in such degenerating neurons. Infrequently encountered TM4-labeled, apparently extracellular NFTs based on their morphology support this assumption (data not shown).

We do not know why iD387 stained only faintly the majority of extracellular NFTs. It is possible that carboxyl-terminal processing of tau could have eliminated isoAsp-387. Nonenzymatic cleavage of tau at this site proceeds for months, as shown by prolonged in vitro incubation of recombinant tau (23). This possibility may be supported by the weak labeling of extracellular NFTs with PHF-1, the epitope of which (phosphoSer-396 and phosphoSer-404) is ~10 residues downstream of Asp-387 (data not shown). Another possibility is that Asp-387 in NFT undergoes further modifications such as racemization (Fig. 1) (36). Related to this, the decreased reactivity of iD387 with dextro-isoAsp-387 is of particular interest (Fig. 2B).

In this study, we hypothesized that TM4-positive NFT counts reflect the generation rate of NFT-bearing neurons. Based on these indices, it is likely that the generation rate is lowest in mild cases, presumably at Braak stages I/II (32). Subsequently, a rather constant generation rate may follow in

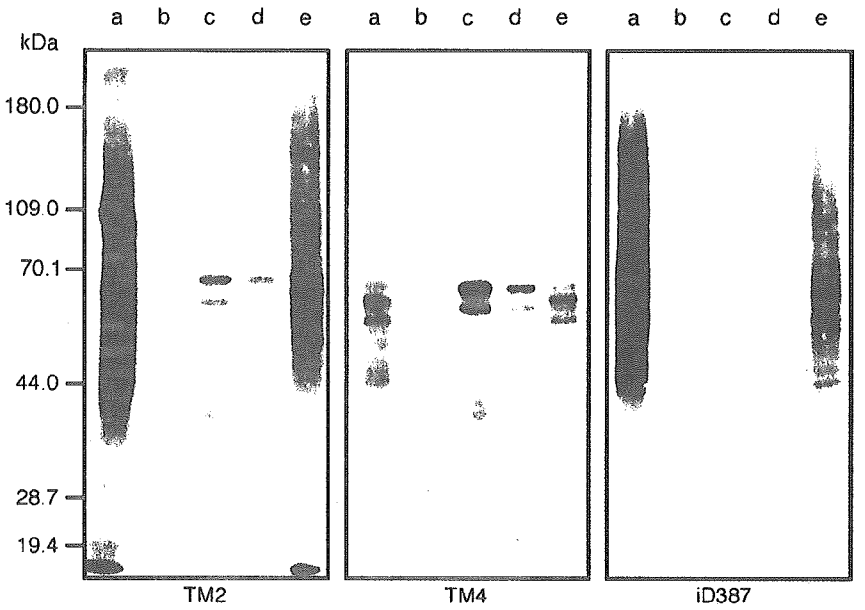

FIGURE 7. IsoAsp formation in the Sarkosyl-insoluble tau in P301L and R406W brains. Sarkosyl-insoluble fractions were prepared from the frontal cortices of one patient with Alzheimer disease (AD) **(a)**, 3 P301L patients **([b]**: 94-075, **[c]**: 94-079, and **[d]**: 96-113), and one R406W patient **([e]**: 99-005), and were subjected to Western blotting using TM2, TM4, and iD387. TM2 detected the PHF smear in AD and R406W cortices, and labeled 2 major bands at 64 and 68 kDa in P301L specimens. iD387 strongly labeled the insoluble smeared tau from an R406W brain, but none from P301L brains. In contrast, TM4 strongly labeled discrete triplet bands in the specimens from AD and R406W brains and 2 bands in the specimens from P301L brains.

moderate to severe cases, which may correspond to Braak stages III to VI. This leads us to postulate the following chronology of NFT formation. In the early phase, tau is slowly deposited in the cytoplasm of large (mostly pyramidal) neuron, likely as pretangles. Presumably, this is the critical period for NFT formation. In Braak stages III/IV, when senile plaques appear in the CA1 region, NFTs are constantly generated and new NFT formation continues until Braak stages V/VI. Finally, NFT-bearing neurons die, and new tau deposition is no longer seen in CA1 neurons at Braak stages V/VI. This assumption can be tested if the 2 antibodies used here were applied to a mouse model showing both amyloid plaques and NFTs (44).

The most striking finding is the differential distribution of Asp-387 and isoAsp-387 in NFTs and NTs in the hippocampus and temporal cortex. Whereas iD387 intensely labeled whole profiles of NFTs up to distal branches of the dendrite, TM4 preferentially stained NFTs in the proximal dendritic portion and perikaryon. This may reflect continued protein biosynthesis in the proximal dendrites and perikarya, and dysfunction of the trafficking required for normal intracellular transport of tau or tau mRNA (45). In the affected neurons, newly synthesized tau or tau mRNA cannot be transported to the distal dendrites and accumulates in the proximal dendrites and cell body, which may further displace intracellular organelles and affect cellular metabolism. This view is supported by repeated observations that tubulin immunoreactivity is completely abolished or displaced to the periphery in NFT-bearing neuronal perikarya (46).

The outer portion of a thread was intensely stained with TM4. Together with the predominant staining of the core portion with iD387, this strongly suggests that NTs constantly gain diameter by addition of newly produced tau (or PHF) on their surface. When NT-containing neurites (mostly dendrites) are disconnected from the cell body, new tau deposition onto NTs ceases and the tau on the outer surface may become gradually deamidated and isomerized. NTs that are exclusively stained with iD387 may represent such a kind of extracellular NTs.

Western blots of specimens from R406W brains showed the presence of isoAsp-387 in the insoluble tau to similar extents as observed in AD brains. This indicates that the NFTs in the R406W brains progressively evolve, and isoAsp-387 increasingly accumulates like in AD brains. In contrast, in P301L brains, none was labeled with iD387. The insoluble tau in P301L brains would be deposited for too short a period for Asp to be converted to isoAsp and cleared rapidly by neuronal death. These may explain the disparity in the clinical and pathologic features of these 2 mutations: P301L is representative of a rapidly progressive phenotype (early onset and short duration), whereas R406W is of a more slowly progressive and mild phenotype (41). Another possible explanation is that the deposited tau, largely mutant P301L tau (34), is structurally weak and swiftly removed by enhanced cellular degradation systems before isoAsp formation, and affected neurons maintain the levels of modified tau very low.

ACKNOWLEDGMENTS

The authors thank Drs. A. Tamaoka and D. J. Selkoe, and M. Yoshimura for providing some of the cases used in this study, and Ms. J. Saishoji and N. Naoi for their technical assistance.

REFERENCES

1. Lee VM, Goedert M, Trojanowski JQ. Neurodegenerative tauopathies. Annu Rev Neurosci 2001;24:1121–59
2. Gomez-Isla T, Hollister R, West H, et al. Neuronal loss correlates with but exceeds neurofibrillary tangles in Alzheimer's disease. Ann Neurol 1997; 41:17–24

3. Braak E, Braak H, Mandelkow EM. A sequence of cytoskeleton changes related to the formation of neurofibrillary tangles and neuropil threads. Acta Neuropathol (Berl) 1994;87:554–67
4. Uchihara T, Nakamura A, Yamazaki M, Mori O. Evolution from pretangle neurons to neurofibrillary tangles monitored by thiazin red combined with Gallyas method and double immunofluorescence. Acta Neuropathol (Berl) 2001;101:535–39
5. Uboga NV, Price JL. Formation of diffuse and fibrillar tangles in aging and early Alzheimer's disease. Neurobiol Aging 2000;21:1–10
6. Brion JP, Hanger DP, Bruce MT, Couck AM, Flament-Durand J, Anderton BH. Tau in Alzheimer neurofibrillary tangles. N- and C-terminal regions are differentially associated with paired helical filaments and the location of a putative abnormal phosphorylation site. Biochem J 1991; 273:127–33
7. Uchihara T, Nakamura A, Yamazaki M, Mori O, Ikeda K, Tsuchiya K. Different conformation of neuronal tau deposits distinguished by double immunofluorescence with AT8 and thiazin red combined with Gallyas method. Acta Neuropathol (Berl) 2001;102:462–66
8. Yen SH, Kress Y. The effect of chemical reagents or proteases on the ultrastructure of paired helical filaments. In: Katzman R, ed. *Biological Aspects of Alzheimer's Disease (Banbury report 15)*. New York: Cold Spring Harbor Laboratory, 1983
9. Selkoe DJ, Ihara Y, Abraham C, Rasool CG, McCluskey AH. Biochemical and immunochemical studies of Alzheimer paired helical filaments. In: Katzman R, ed. *Biological Aspects of Alzheimer's Disease (Banbury Report 15)*. New York: Cold Spring Harbor Laboratory, 1985:125–34
10. Wischik CM, Novak M, Thogersen HC, et al. Isolation of a fragment of tau derived from the core of the paired helical filament of Alzheimer disease. Proc Natl Acad Sci USA 1988;85:4506–10
11. Lee VM. Disruption of the cytoskeleton in Alzheimer's disease. Curr Opin Neurobiol 1995;5:663–68
12. Selkoe DJ, Ihara Y, Salazar FJ. Alzheimer's disease: Insolubility of partially purified paired helical filaments in sodium dodecyl sulfate and urea. Science 1982;215:1243–45
13. Ihara Y, Abraham C, Selkoe DJ. Antibodies to paired helical filaments in Alzheimer's disease do not recognize normal brain proteins. Nature 1983;304:727–30
14. Greenberg SG, Davies P. A preparation of Alzheimer paired helical filaments that displays distinct tau proteins by polyacrylamide gel electrophoresis. Proc Natl Acad Sci USA 1990;87:5827–31
15. Lee VM, Balin BJ, Otvos L Jr., Trojanowski JQ. A68: A major subunit of paired helical filaments and derivatized forms of normal Tau. Science 1991;251:675–78
16. Hasegawa M, Morishima-Kawashima M, Takio K, Suzuki M, Titani K, Ihara Y. Protein sequence and mass spectrometric analyses of tau in the Alzheimer's disease brain. J Biol Chem 1992;267:17047–54
17. Hasegawa M, Watanabe A, Takio K, et al. Characterization of two distinct monoclonal antibodies to paired helical filaments: Further evidence for fetal-type phosphorylation of the tau in paired helical filaments. J Neurochem 1993;60:2068–77
18. Morishima-Kawashima M, Hasegawa M, Takio K, et al. Proline-directed and non-proline-directed phosphorylation of PHF-tau. J Biol Chem 1995; 270:823–29
19. Morishima-Kawashima M, Hasegawa M, Takio K, et al. Hyperphosphorylation of tau in PHF. Neurobiol Aging 1995;16:365-71; discussion 71–80
20. Goedert M, Spillantini MG, Cairns NJ, Crowther RA. Tau proteins of Alzheimer paired helical filaments: Abnormal phosphorylation of all six brain isoforms. Neuron 1992;8:159–68
21. Morishima-Kawashima M, Hasegawa M, Takio K, Suzuki M, Titani K, Ihara Y. Ubiquitin is conjugated with amino-terminally processed tau in paired helical filaments. Neuron 1993;10:1151–60
22. Watanabe A, Takio K, Ihara Y. Deamidation and isoaspartate formation in smeared tau in paired helical filaments. Unusual properties of the microtubule-binding domain of tau. J Biol Chem 1999;274:7368–78
23. Watanabe A, Hong WK, Dohmae N, Takio K, Morishima-Kawashima M, Ihara Y. Molecular aging of tau: Disulfide-independent aggregation and non-enzymatic degradation in vitro and in vivo. J Neurochem 2004;90:1302–11
24. Chazin WJ, Kordel J, Thulin E, Hofmann T, Drakenberg T, Forsen S. Identification of an isoaspartyl linkage formed upon deamidation of bovine calbindin D9k and structural characterization by 2D 1H NMR. Biochemistry 1989;28:8646–53
25. Brennan TV, Anderson JW, Jia Z, Waygood EB, Clarke S. Repair of spontaneously deamidated HPr phosphocarrier protein catalyzed by the L-isoaspartate-(D-aspartate) O-methyltransferase. J Biol Chem 1994;269: 24586–95
26. George-Nascimento C, Lowenson J, Borissenko M, et al. Replacement of a labile aspartyl residue increases the stability of human epidermal growth factor. Biochemistry 1990;29:9584–91
27. Johnson BA, Langmack EL, Aswad DW. Partial repair of deamidation-damaged calmodulin by protein carboxyl methyltransferase. J Biol Chem 1987;262:12283–87
28. Kim E, Lowenson JD, MacLaren DC, Clarke S, Young SG. Deficiency of a protein-repair enzyme results in the accumulation of altered proteins, retardation of growth, and fatal seizures in mice. Proc Natl Acad Sci USA 1997;94:6132–37
29. Yamamoto A, Takagi H, Kitamura D, et al. Deficiency in protein L-isoaspartyl methyltransferase results in a fatal progressive epilepsy. J Neurosci 1998;18:2063–74
30. Fonseca MI, Head E, Velazquez P, Cotman CW, Tenner AJ. The presence of isoaspartic acid in beta-amyloid plaques indicates plaque age. Exp Neurol 1999;157:277–88
31. Goedert M, Spillantini MG, Jakes R, Rutherford D, Crowther RA. Multiple isoforms of human microtubule-associated protein tau: Sequences and localization in neurofibrillary tangles of Alzheimer's disease. Neuron 1989;3:519–26
32. Braak H, Braak E. Neuropathological staging of Alzheimer-related changes. Acta Neuropathol (Berl) 1991;82:239–59
33. Miyasaka T, Morishima-Kawashima M, Ravid R, et al. Molecular analysis of mutant and wild-type tau deposited in the brain affected by the FTDP-17 R406W mutation. Am J Pathol 2001;158:373–79
34. Miyasaka T, Morishima-Kawashima M, Ravid R, Kamphorst W, Nagashima K, Ihara Y. Selective deposition of mutant tau in the FTDP-17 brain affected by the P301L mutation. J Neuropathol Exp Neurol 2001; 60:872–84
35. Schnell SA, Staines WA, Wessendorf MW. Reduction of lipofuscin-like autofluorescence in fluorescently labeled tissue. J Histochem Cytochem 1999;47:719–30
36. Lowenson JD, Clarke S. Recognition of D-aspartyl residues in polypeptides by the erythrocyte L-isoaspartyl/D-aspartyl protein methyltransferase. Implications for the repair hypothesis. J Biol Chem 1992;267: 5985–95
37. Trojanowski JQ, Schuck T, Schmidt ML, Lee VM. Distribution of tau proteins in the normal human central and peripheral nervous system. J Histochem Cytochem 1989;37:209–15
38. Augustinack JC, Schneider A, Mandelkow EM, Hyman BT. Specific tau phosphorylation sites correlate with severity of neuronal cytopathology in Alzheimer's disease. Acta Neuropathol (Berl) 2002;103:26–35
39. Brandt R, Hundelt M, Shahani N. Tau alteration and neuronal degeneration in tauopathies: Mechanisms and models. Biochim Biophys Acta 2005;1739:331–54
40. Goedert M, Jakes R. Mutations causing neurodegenerative tauopathies. Biochim Biophys Acta 2005;1739:240–50
41. van Swieten JC, Stevens M, Rosso SM, et al. Phenotypic variation in hereditary frontotemporal dementia with tau mutations. Ann Neurol 1999;46:617–26
42. Morsch R, Simon W, Coleman PD. Neurons may live for decades with neurofibrillary tangles. J Neuropathol Exp Neurol 1999;58:188–97
43. Bobinski M, Wegiel J, Tarnawski M, et al. Duration of neurofibrillary changes in the hippocampal pyramidal neurons. Brain Res 1998;799:156–58
44. Lewis J, Dickson DW, Lin WL, et al. Enhanced neurofibrillary degeneration in transgenic mice expressing mutant tau and APP. Science 2001;293: 1487–91
45. Litman P, Barg J, Ginzburg I. Microtubules are involved in the localization of tau mRNA in primary neuronal cell cultures. Neuron 1994;13: 1463–74
46. Hempen B, Brion JP. Reduction of acetylated alpha-tubulin immunoreactivity in neurofibrillary tangle-bearing neurons in Alzheimer's disease. J Neuropathol Exp Neurol 1996;55:964–72

J Neuropathol Exp Neurol

Vol. 64, No. 10
October 2005
pp. 1–8

ORIGINAL ARTICLE

Tau-Positive Fine Granules in the Cerebral White Matter: A Novel Finding Among the Tauopathies Exclusive to Parkinsonism–Dementia Complex of Guam

Mineo Yamazaki, MD, PhD, Masato Hasegawa, PhD, Osamu Mori, MD, PhD
Shigeo Murayama, MD, PhD, Kuniaki Tsuchiya, MD, PhD, Kenji Ikeda, MD, PhD
Kwang-Ming Chen, MD, PhD, Yasuo Katayama, MD, PhD, and Kiyomitsu Oyanagi, MD, PhD

Abstract

We examined the autopsied brains of cases of 6 types of tauopathy: parkinsonism–dementia complex of Guam (PDC), corticobasal degeneration (CBD), progressive supranuclear palsy (PSP), Pick disease, Alzheimer disease (AD), and myotonic dystrophy together with Guamanian controls. Light microscopy sections of these brains were examined using anti-tau antibodies. Tau-positive fine granules (TFGs) were globe-shaped, and 3 to 6 μm in diameter, were observed predominantly in the frontal white matter in 30 of the 35 patients with PDC. However, no TFGs were found in association with PSP, myotonic dystrophy, Pick disease, AD, or CBD. Western blot analysis of frozen brain tissue taken from the PDC cases revealed that the frontal cortex was hyperphosphorylated and contained 6 tau isoforms (3R + 4R tau). However, in the present study, it was revealed that the novel TFGs in the white matter of patients with PDC was composed of 4R tau. Western blot analysis of sarkosyl-insoluble tau from the white matter of the PDC cases showed 2 major bands of 60 and 64 kDa and one minor band of 67 kDa. After dephosphorylation, these bands resolved into one major band of 4-repeat (4R) tau isoform and 3 minor bands of 3-repeat (3R) and 4R tau isoforms. Moreover, the TFGs observed in cases in which the number of neurofibrillary tangles (NFTs) was higher than the threshold level were not correlated with the presence of cortical NFTs. In conclusion, these novel TFGs were found almost exclusively in PDC brains and could therefore be considered as a characteristic neuropathologic marker of this particular tauopathy. The TFGs were hyperphosphorylated tau-positive structures that may be formed by a different mechanism from that used to produce cortical NFTs.

Key Words: Alzheimer disease, Corticobasal degeneration, Myotonic dystrophy, Parkinsonism–dementia complex of Guam, Pick disease, Tauopathies.

INTRODUCTION

Accumulations of hyperphosphorylated tau protein in neurons or glial cells are the hallmark lesions of a subset of neurodegenerative disorders that include corticobasal degeneration (CBD), progressive supranuclear palsy (PSP), Pick disease, Alzheimer disease (AD), argyrophilic grain disease (AGD), frontotemporal dementia with parkinsonism linked to chromosome 17 (FTDP-17) (1), and parkinsonism–dementia complex of Guam (PDC). These are referred to collectively as tauopathies. Biochemical and immunohistochemical analyses of tauopathy brains have shown that the morphologically distinct inclusions consist of either all 6 brain tau isoforms or the 3R tau or 4R tau isoforms only, depending on the disease (2).

Severe cerebral cortical atrophy is observed in the gray matter of PDC brains, as well as neuronal loss predominantly in the temporal and frontal lobes, and numerous neurofibrillary tangles (NFTs) with a distribution similar to that observed in AD brains (3, 4). The distribution of cortical NFTs predominantly in layers II and III in PDC brains is similar to that seen in PSP (5). The presence of granular hazy astrocytes has been reported by Oyanagi et al to be a specific neuropathologic marker of PDC (6). Thus far, no other specific marker for PDC has been found.

In contrast to the small number of tau-positive glial inclusions observed in the AD white matter, the PDC brains contained a substantial population of tau-positive glial inclusions such as argyrophilic threads, coiled bodies, and granular hazy astrocytes. During a precise examination of the PDC white matter, we observed tau-positive fine granules (TFGs). We investigated whether these structures were universal in all patients with PDC and examined whether they are specific to this particular tauopathy. Moreover,

From the Department of Neuropathology (MY, KO), Tokyo Metropolitan Institute for Neuroscience, Fuchu-shi, Tokyo; Department of Neurology (MY, YK) and 2nd Department of Pathology (OM), Nippon Medical School, Bunkyo-ku, Tokyo; Departments of Molecular Neurobiology (MH) and Psychogeriatrics (KI), Tokyo Institute of Psychiatry, Setagaya-ku, Tokyo; Department of Neuropathology (SM), Tokyo Metropolitan Institute of Gerontology, Itabashi-ku, Tokyo; Department of Laboratory Medicine and Pathology (KT), Tokyo Metropolitan Matsuazwa Hospital, Setagaya-ku, Tokyo, Japan; and Department of Neurology (K-MC), Guam Memorial Hospital, Guam.

Send correspondence and reprint requests to: Dr. Mineo. Yamazaki, Department of Neuropathology, Tokyo Metropolitan Institute for Neuroscience, 2-6 Musashidai, Fuchu-shi, Tokyo 183-8526, Japan; E-mail: yamazaki@nms.ac.jp

This work was supported in part by a grant from the Japanese Ministry of Health, Labor and Welfare, Research on Psychiatric and Neurological Diseases (H16-kokoro-017) and a Grant-in-Aid for Research in Priority Areas from the Japanese Ministry of Education, Culture, Sports, Science and Technology (MH).

JOBNAME: jnen 64#10 2005 PAGE: 2 OUTPUT: Wed August 31 05:54:36 2005
lww/jnen/101735/NEN200025

a biochemical analysis of tau proteins in the white matter from patients with PDC was carried out to elucidate whether these TFGs are biochemically different from other tau-positive constituents.

MATERIALS AND METHODS

Cases

The present study was carried out using brains taken at autopsy from patients with PDC (n = 35), Guamanian PDC with amyotrophic lateral sclerosis (ALS; n = 4), Guamanian ALS (n = 7), Guamanian nonPDC, nonALS controls with neurologic disorders (n = 11), CBD (n = 10), PSP (n = 15), Pick disease (n = 4), AD (n = 10), AGD (n = 5), and myotonic dystrophy (n = 5; Table). Myotonic dystrophy was known to have NFTs in the neocortex and in subcortical nuclei (7). All of the Guamanian cases were examined and their condition diagnosed clinicopathologically by the authors (8–13). Some of the clinical and neuropathologic findings of the cases of CBD, PSP, Pick disease, AD, AGD, and myotonic dystrophy have already been reported elsewhere (14–26).

Histochemistry and Immunohistochemistry

The frontal white matter from autopsied brain tissue was cut into blocks, fixed in formalin, embedded in paraffin, and then sectioned at 4 μm. Some of these sections were stained with hematoxylin and eosin and by the Kluver-Barrera and Gallyas-Braak methods. The remaining sections were incubated with one of the following primary antibodies: anti-tau (AT8, monoclonal, 1:1000; Innogenetics, Temse, Belgium), anti-human tau (a gift from Professor Ihara, 1:1000; [27]), anti-ubiquitin (polyclonal, rabbit, 1:1000; Dako), and anti-glial fibrillary acidic protein (GFAP, polyclonal, rabbit, 1:1000; Dako). The immunolabeled sections were observed with the aid of a fluorescence microscope combined with a laser confocal system (TCS-SP; Leica, Heidelberg, Germany). For double immunostaining with anti-paired helical filaments (PHF) tau monoclonal (AT8, 1:1000; Innogenetics) and anti-GFAP/anti-ubiquitin/anti-phosphorylated neurofilaments (SMI31) antibodies, the specimens were blocked with nonimmune sera from horse or goat, depending on the secondary antibody used. Sections were first incubated with a mixture of the 2 primary antibodies and then with the fluorescence-labeled secondary antibodies (i.e. anti-mouse IgG coupled with fluorescein isothiocyanate [1:200; Cappel, Irvine, CA] and anti-rabbit IgG coupled with rhodamine [1:200; Cappel]).

TABLE. Summary of Cases Examined in This Study

Disease	Number	Gender of Cases	Age (years)
PDC of Guam (died 1979–1982)	35	23 male/2 female	64.4 ± 8.32
Guam PDC-ALS	4	2 male/2 female	63.0 ± 6.06
Guam ALS	7	3 male/4 female	52.1 ± 10.0
Guam control	11	4 male/7 female	68.8 ± 11.5
Corticobasal degeneration	10	4 male/6 female	65.7 ± 5.43
Progressive supranuclear palsy	15	8 male/7 female	74.4 ± 8.82
Pick disease	4	2 male/2 female	71.5 ± 3.70
Alzheimer disease	10	1 male/9 female	74.6 ± 15.1
Argyrophilic grain disease	5	3 male/2 female	82.4 ± 7.92
Myotonic dystrophy	5	3 male/2 female	54.4 ± 19.7

PDC, Parkinsonism–dementia complex; ALS, amyotrophic lateral sclerosis.

Quantitative Examination of Neurofibrillary Tangles and Tau-Positive Fine Granules

We performed quantitative analyses on the frontal subcortical white matter of brains from clinically diagnosed patients with PDC. The relationship between NFTs and TFGs was clarified by calculating the density of NFTs and TFGs in the frontal cortex of 12 patients with PDC. These 12 patients were sampled randomly from the 35 PDC cases examined in this study. With the aid of Gallyas-Braak staining, we computed the density of NFTs, including pretangles, in all layers of the 100-μm-wide frontal cortical ribbon. The number of TFGs in the center of the centrum semiovale in the frontal white matter was calculated by summing the number of TFGs in evenly distributed serial fields measuring 2.5 μm × 2.5 μm (giving a total area of 6.25 μm^2). The correlation between the density of NFTs and that of TFGs was estimated using Spearman's rank correlation coefficient. We used the Kruskal-Wallis test for comparing the density of NFTs with that of TFGs. Differences at $p < 0.05$ were considered significant.

Immunoelectron Microscopy

Paraffin-embedded, 6-μm-thick sections from the cerebral frontal white matter of PDC cases with tau-positive TFGs were immunostained with anti-tau antibody (AT8). The immunolabeling was visualized with diaminobenzidine (DAB), like for light microscope immunohistochemistry, and then processed for immunoelectron microscopy. After being post-fixed in 4% OsO_4 for 15 minutes, the sections were dehydrated in a graded ethanol series, embedded in epon 812, and then polymerized at 60°C for 24 hours. Ultrathin sections were cut and then stained with 3% lead acetate for 2 minutes and viewed with an electron microscope (H-9000; Hitachi, Japan) (28).

Biochemical Analysis

Frozen brain tissues from the frontal region, including both the gray matter and deep white matter of 4 PDC cases, one Guamanian ALS case with abundant TFGs in both the gray and white matter, one Guamanian control case, and 2 classic AD cases, were used for biochemical analysis. All of these brains were frozen at autopsy at −80°C. The gray and white matters were separated from each other macroscopically. Sarkosyl-insoluble tau was prepared according to a modification of the method of Goedert et al (29). Tissues were homogenized in a 10-fold (v/w) dilution of extraction buffer (10 mM Tris-HCl [pH 7.5], 1 mM EGTA, 0.8 M NaCl, 10% sucrose) and centrifuged at 23,000 × *g* for 20 minutes at 4°C. The pellets were rehomogenized in extraction buffer. Both of the 23,000 × *g* supernatants were combined, brought to 1% sarkosyl, and incubated for 1 hour at room temperature. After centrifugation at 113,000 × *g* for 20 minutes at 25°C, the

pellets were resuspended in 7 M guanidine-HCl and then dialyzed overnight against 30 mM Tris-HCl (pH 8.8). Dephosphorylation and immunoblotting were performed as described previously (30).

RESULTS

Microscope Study

The cerebral white matter of most patients with PDC exhibited no evident pallor with Kluver-Barrera stain. In addition to the TFGs, in the white matter of PDC (Fig. 1A, C), we found some tau-positive argyrophilic threads and coiled bodies. Some tiny tau-positive granular or thread-like structures with a diameter of 1 to 3 μm were also found in the PDC brains and in those of the other tauopathies studied here (Fig. 1B, D). These thread-like structures were found mainly in the frontal and temporal white matter and were not specific to PDC. They were also observed in the white matter of brains from patients with the other tauopathies examined in this study (AGD and CBD brain) and were clearly distinct from TFGs (Fig. 2A, B).

We observed TFGs in the frontal white matter of 30 of 35 patients with PDC (86%) and in 3 of 4 patients with PDC-ALS (75%). Moreover, only one of 7 Guamanian patients with ALS (14%) and 2 of 11 Guamanian controls (18%) whose cerebral cortices exhibited many NFTs also exhibited TFGs (Fig. 3). However, no TFGs were found in the brains of patients with myotonic dystrophy, Pick disease, or AD. In CBD brains, we found large numbers of argyrophilic threads and coiled bodies, but no TFGs (Fig. 2B). The TFGs were globe-shaped and approximately 3 to 6 μm in diameter, and were distinct from argyrophilic threads. TFGs were positive to both AT8 and anti-human tau antibodies (Fig. 1A, B), but some parts of them were not stained by the Gallyas-Braak method. Some TFGs consisted of globular dense tau-positive structures surrounded by weakly tau-positive fluffy materials (Fig. 1C). They were observed frequently in the frontal white matter, the frontal lobe, and the temporal subcortical white matter. In the PDC cases in which TFGs were abundant in the frontal white matter, some were also found in the frontal cortex. However, TFGs were only rarely observed in the spinal cord, cerebellum, or brainstem.

Confocal scanning microscope observations of immunofluorescence double-labeled sections showed that GFAP and phosphorylated neurofilament were not localized on TFGs (Fig. 4A, B). Although most of the TFGs exhibited no colocalization of ubiquitin and tau, it was observed on some (Fig. 4C). The pattern of this colocalization, when it was observed, varied from only a small part (i.e. the center) of the TFG to staining in almost all of it.

Quantitative Analysis of Tau-Positive Fine Granules and Neurofibrillary Tangles

We found no significant relationship between the number of NFTs and the number of TFGs. However, the 12 patients with PDC could be divided into 2 groups: those with more than 200 NFTs/100 μm-length of the frontal cortical ribbon and those with less (Fig. 5). The graph shown in Figure 4 shows that TFGs were only observed in those PDC cases with more than approximately 200 NFTs/100 μm-length of the frontal cortical ribbon. There was no significant correlation between the degree of white matter degeneration and the density of TFGs.

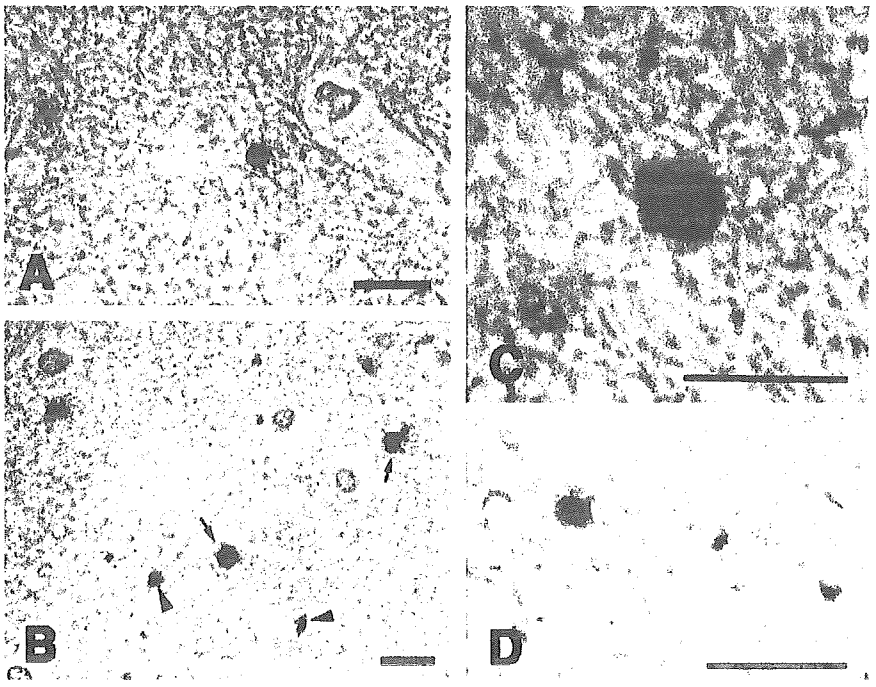

FIGURE 1. Immunohistochemical findings in the frontal white matter of parkinsonism–dementia complex of Guam (PDC) brains. Anti-tau antibodies (human tau [A] and AT8 [B]) were used to examine sections of the frontal white matter. **(B)** Tau-positive fine granules (TFGs) (arrows) are globe-shaped and approximately 3 to 6 μm in diameter, and are distinct from argyrophilic threads. They were observed frequently in the frontal white matter. Tiny tau-positive granular structures (arrowheads) of 1 to 3 μm in diameter were found in the PDC brains and those of other tauopathies. These structures are thus not specific to PDC and could be clearly distinguished from TFGs. High-power views of TFGs **(C)** and tiny tau-positive granular structures **(D)**, both stained immunohistochemically for tau using AT8. **(C)** Some TFGs consisted of globular dense tau-positive structures surrounded by weakly tau-positive fluffy materials. Scale bars: 10 μm.

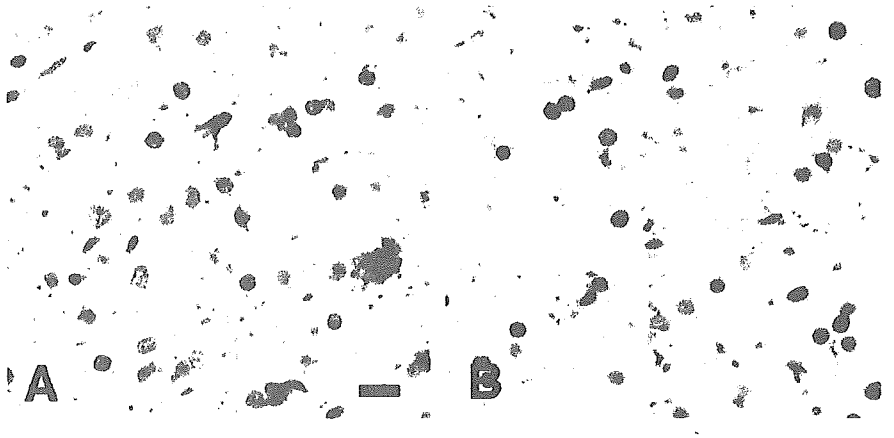

FIGURE 2. Immunohistochemical findings in the frontal white matter of brains with argyrophilic grain disease (AGD) **(A)** and corticobasal degeneration (CBD) **(B)** using anti-tau (AT8) antibody. Abundant tiny tau-positive granular structures were found, but no tau-positive fine granules were observed found in the frontal white matter of brains with AGD **(A)** and CBD **(B)**. Scale bars: 10 μm.

Immunoelectron Microscope Observations

Most of the AT8-positive TFGs had some contact with the myelin outer loop, but no TFGs were observed within the myelin sheath or the axons (Fig. 6A). High-power views of these sections revealed that TFGs contained round structures that were 20 to 30 nm in diameter (including the DAB substrate) (Fig. 6B). These structures were also observed near the nucleus of glial cells that were thought to be oligodendroglia (Fig. 6C, D).

Biochemical Analysis

The sarkosyl-insoluble fraction prepared from the white matter of the frontal lobes of PDC cases that exhibited TFGs were analyzed by Western blotting with a the phosphorylation-independent anti-tau antibody HT-7. Two major bands were detected, one with an apparent molecular mass of 60 kDa and another of 64 kDa, and one minor band with an apparent molecular mass of 68 kDa. After dephosphorylation, these bands appeared as one major band corresponding to a 4-repeat tau isoform with zero amino acid inserts (4R0N) and 3 minor bands corresponding to a 4-repeat tau isoform with 29 amino acid inserts (4R29N), a 3-repeat tau isoform with zero amino acid inserts (3R0N), and a 3-repeat tau isoform with 29 amino acid inserts (3R29N; Fig. 7).

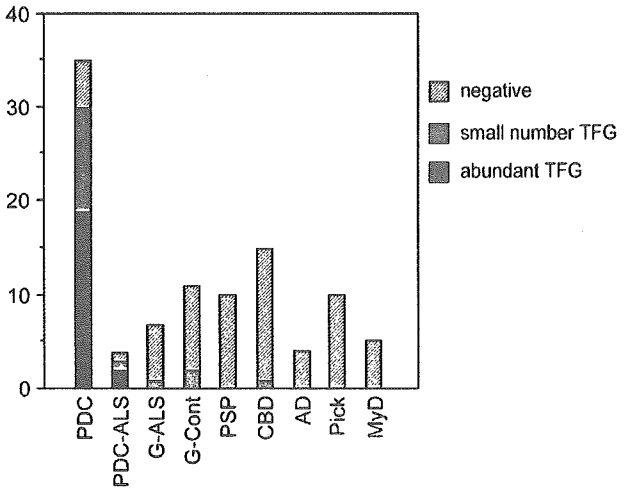

FIGURE 3. Tau-positive fine granules (TFGs) in the frontal white matter of brains with various tauopathies. Histogram showing the number of the cases having abundant TFGs (black), cases with only a small number of TFGs (narrow slash mark), and TFG-negative cases (broad slash mark) in each disease group. The density 50 TFGs/100 μm^2 marked the border between the "abundant TFGs" group and the "small number of TFGs" group. PDC, Parkinsonism–dementia complex; G-ALS, Guam amyotrophic lateral sclerosis; G-Cont, Guam control; CBD, corticobasal degeneration; PSP, progressive supranuclear palsy; AD, Alzheimer disease; Pick, Pick disease; MyD, myotonic dystrophy.

The insoluble tau extracted from the gray matter of cortices from the PDC cases resolved into 3 bands of apparent molecular mass 60, 64, and 68 kDa. Six bands were detected after dephosphorylation, corresponding to 6 tau isoforms that resembled those that were resolved in AD brains. Similar results were obtained from the analysis of another PDC case (PDC-4) and one Guamanian ALS case with abundant TFGs (data not shown). No insoluble tau was extracted from the frontal brain of a Guamanian control. Accumulations of both 3R and 4R tau isoforms were detected in the white matter of the PDC cases. However, when compared with tau in the gray matter, the levels of 4R tau isoforms were high and the levels of 3R tau isoforms were very low, which was different from those in the gray matter in which similar levels of 3R and 4R tau isoforms or slightly higher levels of 3R tau isoforms were detected. Furthermore, the 4R tau band pattern after dephosphorylation was most obvious in cases in which TFGs were abundant in the white matter. These results suggest that the TFGs in the white matter in the patients with PDC were composed predominantly of 4R tau isoforms. The difference of band pattern of tau between gray matter and white matter was clearly shown from these data of Western blotting after dephosphorylation, that is, the 4 major bands with equal levels of 3R and 4R tau isoforms or slightly higher levels of 3R29N band in gray matter and one major 4R0N band and 3 minor 4R and 3R tau bands in the white matter. The ratio of 4R tau isoforms to the 3R tau isoforms in white matter was different from that in the gray matter of PDC brains.

Sarkosyl-insoluble tau from the white matter of AD brains consisted of a triplet of apparent molecular mass 60, 64, and 68 kDa, which resolved into 6 bands after

JOBNAME: jnen 64#10 2005 PAGE: 5 OUTPUT: Wed August 31 05:54:51 2005
lww/jnen/101735/NEN200025

dephosphorylation (data not shown), indicating that in AD, the tau isoforms deposited in the white matter (mostly in axons) were the same as those deposited in the gray matter, although there was far less of the pathologic tau in the white matter than in the gray matter.

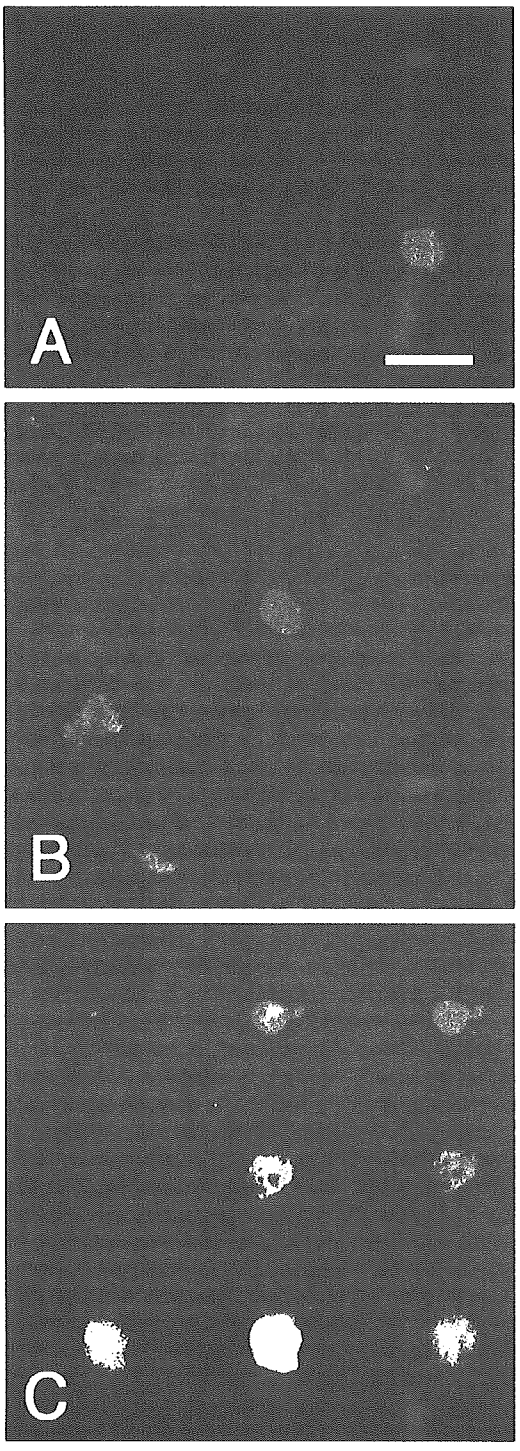

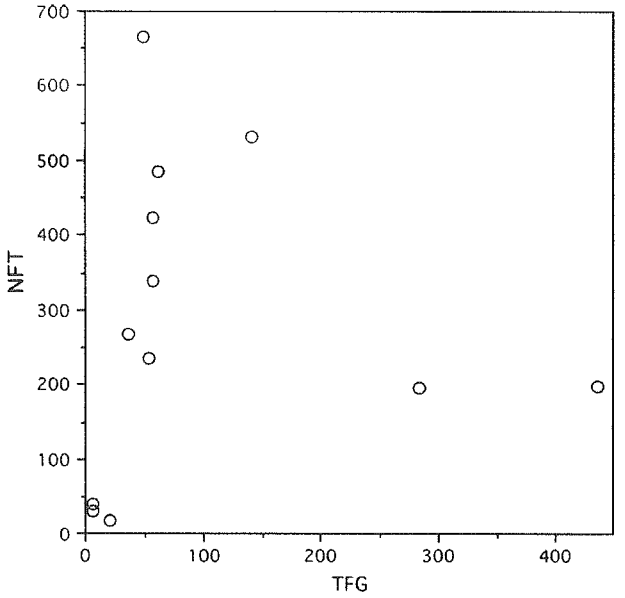

FIGURE 5. Relationship between the densities of neurofibrillary tangles (NFTs) and tau-positive fine granules (TFGs) in Guam parkinsonism–dementia complex (PDC). The number of TFGs was counted in a 100-μm^2 area of frontal white matter and the number of NFTs was counted in a 100-μm length of the frontal cortex. No significant relationship was found between the numbers of NFTs and TFGs in the frontal brains of patients with Guam PDC. However, it is safe to say that TFGs only seem to develop when the number of NFTs reaches a certain threshold level.

DISCUSSION

TFGs are novel and unique tau-positive inclusions that we observed in the frontal white matter of 86% of the patients with PDC examined here. No TFGs were found in the brains of patients with myotonic dystrophy, Pick disease, or AD. Furthermore, only a few of the Guamanian controls and Guamanian patients with ALS with many NFTs also exhibited TFGs. Globe-shaped and tau-positive inclusions like TFGs have never been described previously, although other tau-positive inclusions have been reported. Immunoelectron microscope observations revealed that putative TFGs are tau-positive structures that take the shape of granules with a diameter of 20 to 30 nm (including the DAB coating). The PDC white matter stained with Kluver-Barrera and Bodian did not mark a significant change in the stainability even in cases with many TFGs, despite atrophy of the white matter TFGs might relate

FIGURE 4. Confocal scanning microscope observations made with the aid of immunofluorescence double labeling. GFAP ([A], green) and phosphorylated neurofilament ([B], green; SMI 31) were not localized on tau-positive fine granules (TFGs) (red; AT8). (C) Ubiquitin (green; left) was localized with tau (AT8, red; right) on TFGs in various distribution patterns (merged images) from only a small part (center) of the TFG to staining throughout most of the TFG (lower stand). Scale bars: 5 μm.

Fig. 4 live 4/C

JOBNAME: jnen 64#10 2005 PAGE: 6 OUTPUT: Wed August 31 05:55:01 2005
lww/jnen/101735/NEN200025

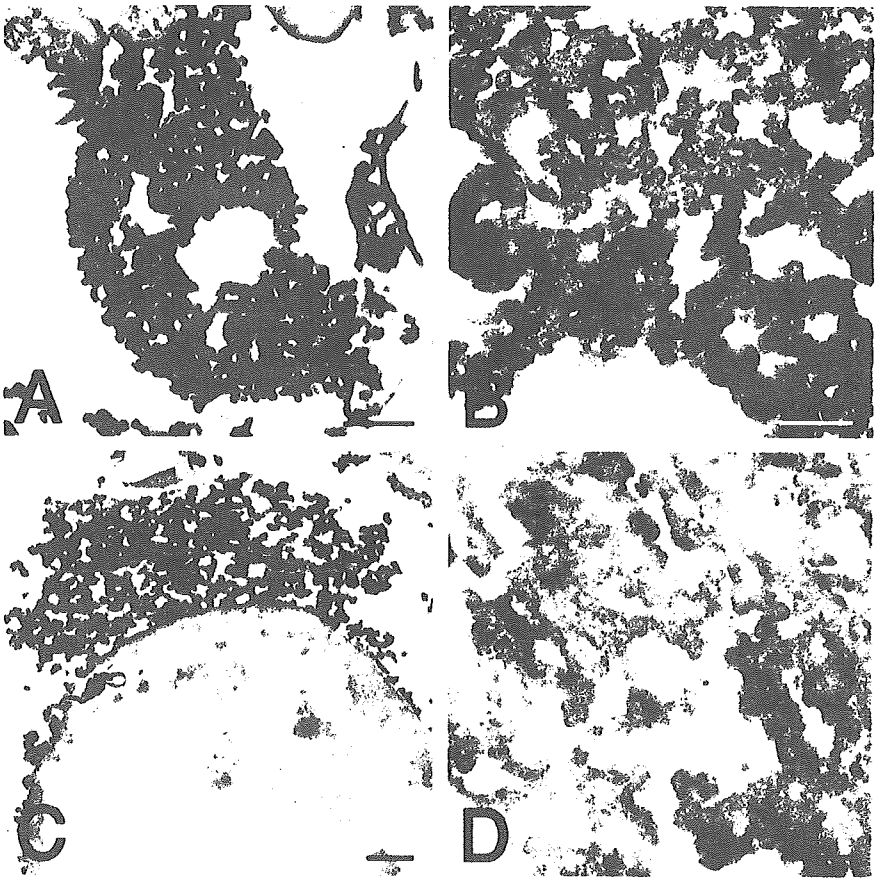

FIGURE 6. Immunoelectron microscope analysis of tau-positive fine granules (TFGs). **(A)** AT8-positive TFGs had no contact with the myelin outer loop (arrow) and no TFGs were observed either within the myelin sheath itself or the axons. **(B)** Examination of high-power views revealed that TFGs are permeated by round structures that are 20 to 30 nm in diameter (including the DAB substrate). **(C, D)** Similar structures were observed near the nucleus of the glial cells that were thought to be oligodendroglia. Scale bars = **(A, C)** 300 nm; **(B, D)** 100 nm.

to this peculiar degeneration of the PDC white matter. We became interested in whether the presence of TFGs had a connection to the atrophy of white matter in the PDC brain.

Immunofluorescence double labeling of TFGs, observed with the aid of confocal scanning microscopy, revealed no colocalization of GFAP and tau staining or of phosphorylated neurofilament and tau staining on these structures. Therefore, it is unlikely that TFGs originate from either astrocytes or axons. TFGs that were closely associated with the outer layer of the myelin sheath were occasionally bordered by the nucleus of what appeared to be oligodendroglia. It is thus likely that TFGs are derived from oligodendroglia.

Many abnormal tau-positive structures in oligodendroglial cells such as ATs and coiled bodies have been observed in human brains (31–34). These structures are invariably observed in brains with CBD and PSP, but are not specific to neurodegenerative disorders. There are no previous reports of disease-specific oligodendroglial tau-positive inclusions that are a pathologic marker for tauopathies. Numerous tau-positive structures have been observed in the white matter of CBD brains (35, 36), and it is difficult to state categorically that no TFGs exist in the CBD white matter. However, none were observed in the CBD brains that were examined in the present study. TFGs bear a striking resemblance to argyrophilic grains morphologically, but the distribution of argyrophilic grains is quite different from that of TFGs. In AGD, argyrophilic grains are observed in cerebral cortex, amygdala, hypothalamus, and claustrum, but the deep white matter of frontotemporal lobes does not contain argyrophilic grains (37). In this study, tiny thread-like structures were also observed in the vicinity of TFGs in PDC. However, these structures were also detected in brains with CBD, PSP, Pick disease, AGD, and AD.

These structures are therefore not specific to any one tauopathy. Recently, Powers et al reported a case with novel leukoencephalopathy associated with tau deposits primarily in the glia of the white matter (38). In this case, tau-positive structures similar to TFGs were observed mainly in the frontal white matter. However, ultrastructurally, these tau deposits look completely different from TFGs, appearing in the form of straight filaments with a diameter of approximately 10 nm.

In Guam, cases of PDC with many NFTs also had many TFGs in the white matter, whereas in those cases with relatively small numbers of NFTs, TFGs were observed only rarely. Similarly, controls and cases of ALS with few NFTs had a small number of TFGs. Thus, it appears that TFGs only develop when the number of NFTs reaches a certain threshold. However, on further investigation, we found no significant lineal correlation between the presence of TFGs and the number of NFTs and granular hazy astrocytes (6). In addition, NFTs are known to be involved in fibril formation, but we

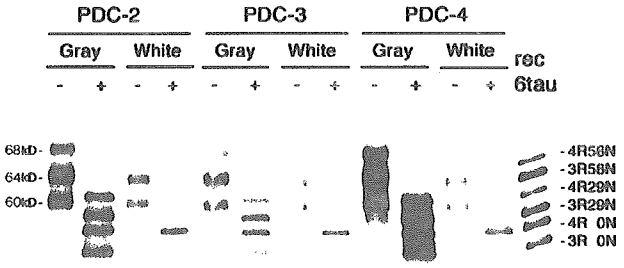

FIGURE 7. Western blot analysis of sarkosyl-insoluble tau from the frontal lobe of parkinsonism–dementia complex of Guam cases stained with the phosphorylation-independent anti-tau antibody, HT-7. HT-7 immunohistochemistry immunoblotting revealed the presence of 2 major bands of relative molecular mass 60 and 64 kDa, and one minor band of 68 kDa. After dephosphorylation, these bands appeared as one major band corresponding to a 4-repeat tau isoform with zero amino acid inserts (4R0N), 3 minor bands corresponding to a 4-repeat tau isoform with 29 amino acids inserts (4R29N), a 3-repeat tau isoform with zero amino acid inserts (3R0N), and a 3-repeat tau isoform with 29 amino acid inserts (3R29N). Recombinant tau isoforms were confined to the right side. Gray = gray matter; white = white matter.

found no fibrils in the TFGs. These results suggest that in Guam PDC brains, the mechanisms of tau deposition underlying the formation of NFTs and TFGs are different.

The presence of TFGs in patients with Guam PDC and Guam ALS does not prove that Guam ALS is a different disease from classic ALS or that Guam PDC and Guam ALS represent a single disease entity. The number of TFGs in many patients with Guam ALS was similar to that in nonPDC, nonALS control subjects. This finding indicates that TFGs are typical features of the general Guamanian population, as is the case with NFTs and granular hazy astrocytes. Moreover, our biochemical analysis revealed that the tau in the white matter of Guam PDC brains is composed of 4R tau. Some previous reports have shown that the tangles present in AD and PDC brains share the same profile when examined immunohistochemically with antihyperphosphorylated tau antibodies, and all 6 tau isoforms have been observed in tangle formation in Guamanian PDC as well as in AD brains (39, 40). A biochemical study of PDC brains in from individuals living on the Kii Peninsula also revealed that the dephosphorylated PHF tau protein is composed of all 6 isoforms (41). Until now, a regional biochemical analysis of tau proteins had not been carried out, and the present study represents the first biochemical analysis of the white matter of PDC brains (42–47). The results presented here show clearly that after dephosphorylation, the extracted insoluble tau is composed predominantly of the 4R tau isoforms, and that all 6 isoforms can be found in the frontal cortex (gray matter).

In recent years, it has been shown that the tau in sporadic Pick disease (48, 49) and in hereditary FTDP-17 (L266V) is composed of more than one tau isoform (3R and 4R tauopathies) (50). In the study presented here, it has been demonstrated that in Guamanian PDC, there are 2 distinct patterns of tau isoform composition; all 6 tau isoforms occur in the cerebral cortex and the 4R tau isoforms predominantly occur in the cerebral white matter. This is the first report of the existence of this combination of tau isoforms. Because the 4R tau (predominant) pattern was most obvious in cases in which TFGs were abundant in the white matter, these 4R tau isoforms are thought to reflect the biochemical characteristics of TFG. This raises the possibility that tau accumulates in those neurons expressing both 3R tau and 4R tau in the cerebral cortex and that tau builds up in those glial cells expressing 4R tau in the white matter. These glial cells exhibited tau isoform patterns such as 4R0N major, 4R29N, 3R0N, and 4R0N minor. Only one pattern of tau isoform was expressed in any one cell type, and the isoform of accumulated tau was dependent on which cells were involved in the lesions.

In a recent study, "tau-immunoreactive inclusions in glial cells in the white matter" resembling TFGs have been reported in cases with "primary progressive aphasia as the initial manifestation of corticobasal degeneration and unusual tauopathies" (51). Although these globular glial inclusions in the white matter are very similar to TFGs in Guamanian PDC, their size is reportedly larger than that of TFGs. In addition, the Western blotting analysis of total brain homogenates carried out in the present study showed 2 bands of relative molecular mass 68 and 64 kDa, in common with CBD but differing from Guam PDC white matter. It is hoped that these "tau-immunoreactive glial inclusions in the white matter" will be investigated further with the aid of immunoelectron microscopy.

In this study, TFGs were found exclusively in PDC brains and could therefore be a characteristic neuropathologic marker of this disease. The tau isoform in the gray matter (3R + 4R tau) was different from that in the white matter (4R tau) in PDC. This difference is thought to be a function of the cell type from which the tau originated. If this is the case, the question remains as to why particular tau isoforms prevail in the different cell types in any particular brain region and what mechanism underlies this process. The mechanism underlying disease-specific and tau-positive ultrastructural formations should be clarified in accordance with their particular tau isoform.

ACKNOWLEDGMENTS

The authors thank Dr. H. Takahashi, Department of Neuropathology, Graduate School of Medicine, Niigata University; and Ms. E. Kawakani, Department of Neuropathology, Tokyo Metropolitan Institute for Neuroscience, for their cooperation in this research.

REFERENCES

1. Spillantini MG, Murrell JR, Goedert M, et al. Mutation in the tau gene in familial multiple system tauopathy with presenile dementia. Proc Natl Acad Sci U S A 1998;95:7737–41
2. Spillantini MG, Goedert M. Tau protein pathology in neurodegenerative disease. Trends Neurosci 1998;21:428–33
3. Hirano A, Malamud N, Kurland LT. Parkinsonism–dementia complex, an endemic disease on the island of Guam. II. Pathological features. Brain 1961;84:662–79
4. Hof PR, Perl DP, Loerzel AJ, Morrison JH. Neurofibrillary tangle distribution in the cerebral cortex of parkinsonism–dementia cases from Guam: Differences with Alzheimer's disease. Brain Res 1991;564:306–13
5. Hof PR, Delacourte A, Bouras C. Distribution of cortical neurofibrillary tangles in progressive supranuclear palsy: A quantitative analysis of six cases. Acta Neuropathol (Berl) 1992;84:45–51

6. Oyanagi K, Makifuchi T, Ohtoh T, et al. Distinct pathological features of the Gallyas- and tau-positive glia in the parkinsonism–dementia complex and amyotrophic lateral sclerosis of Guam. J Neuropathol Exp Neurol 1997;56:308–16
7. Vermersch P, Sergeant N, Ruchoux MM, et al. Specific tau variants in the brains of patients with myotonic dystrophy. Neurology 1996;47:711–17
8. Oyanagi K, Wada M. Neuropathology of parkinsonism–dementia complex and amyotrophic lateral sclerosis of Guam: An update. J Neurol 1999; 246(suppl 2):II19–27
9. Oyanagi K, Makifuchi T, Ohtoh T, et al. Topographic investigation of brain atrophy in parkinsonism–dementia complex of Guam: A comparison with Alzheimer's disease and progressive supranuclear palsy. Neurodegeneration 1994;3:301–4
10. Oyanagi K, Makifuchi T, Ohtoh T, et al. The neostriatum and nucleus accumbens in parkinsonism-dementia complex of Guam: A pathological comparison with Alzheimer's disease and progressive supranuclear palsy. Acta Neuropathol (Berl) 1994;88:122–28
11. Oyanagi K, Makifuchi T, Ohtoh T, et al. Amyotrophic lateral sclerosis of Guam: The nature of the neuropathological findings. Acta Neuropathol (Berl) 1994;88:405–12
12. Oyanagi K, Tsuchiya K, Yamazaki M, Ikeda K. Substantia nigra in progressive supranuclear palsy, corticobasal degeneration, and parkinsonism–dementia complex of Guam: Specific pathological features. J Neuropathol Exp Neurol 2001;60:393–402
13. Wada M, Uchihara T, Nakamura A, Oyanagi K. Bunina bodies in amyotrophic lateral sclerosis on Guam: A histochemical, immunohistochemical and ultrastructural investigation. Acta Neuropathol (Berl) 1999;98:150–56
14. Oda T, Kogure T, Tominaga I, et al. An autopsy case of progressive supranuclear palsy with echolalia showing psychiatric symptoms at the beginning. J Clin Psychiatry 1994;36:1159–66
15. Tsuchiya K, Miyazaki H, Ikeda K, et al. Serial brain CT in corticobasal degeneration: Radiological and pathological correlation of two autopsy cases. J Neurol Sci 1997;152:23–29
16. Tsuchiya K, Uchihara T, Oda T, et al. Basal ganglia lesions in corticobasal degeneration differ from those in Pick's disease and progressive supranuclear palsy. A topographic neuropathological study of six autopsy cases. Neuropathology 1997;17:208–16
17. Tsuchiya K, Ikeda K, Uchihara T, et al. Distribution of cerebral cortical lesions in corticobasal degeneration: A clinicopathological study of five autopsy cases in Japan. Acta Neuropathol 1997;94:416–24
18. Tsuchiya K, Ikeda M, Hasegawa K, et al. Distribution of cerebral cortical lesions in Pick's disease with Pick bodies: A clinicopathological study of six autopsy cases showing unusual clinical presentations. Acta Neuropathol (Berl) 2001;102:553–71
19. Tsuchiya K, Ishizu H, Nakano I, et al. Distribution of basal ganglia lesions in generalized variant of Pick's disease: A clinicopathological study of four autopsy cases. Acta Neuropathol (Berl) 2001;102:441–48
20. Tsuchiya K, Ikeda K. Basal ganglia lesions in 'Pick complex': A topographic neuropathological study of 19 autopsy cases. Neuropathology 2002;22:323–36
21. Arai T, Ikeda K, Akiyama H, et al. Distinct isoforms of tau aggregated in neurons and glial cells in brains of patients with Pick's disease, corticobasal degeneration and progressive supranuclear palsy. Acta Neuropathol (Berl) 2001;101:167–73
22. Ikeda K, Akiyama H, Iritani S, et al. Corticobasal degeneration with primary progressive aphasia and accentuated cortical lesion in superior temporal gyrus: Case report and review. Acta Neuropathol (Berl) 1996;92:534–39
23. Arai Y, Yamazaki M, Mori O, et al. α-Synuclein-positive structures in cases with sporadic Alzheimer's disease: Morphology and its relationship to tau aggregation. Brain Res 2001;888:287–96
24. Yamazaki M, Nakano I, Imazu O, et al. Astrocytic straight tubules in the brain of a patient with Pick's disease. Acta Neuropathol (Berl) 1994;88:587–91
25. Yamazaki M, Nakano I, Imazu O, Terashi A. Paired helical filaments and straight tubules in astrocytes: An electron microscopic study in dementia of the Alzheimer type. Acta Neuropathol (Berl) 1995;90:31–36
26. Saito Y, Nakahara K, Yamanouchi H, Murayama S. Severe involvement of ambient gyrus in dementia with grains. J Neuropathol Exp Neurol 2002;61:789–96
27. Ihara Y. Massive somatodendritic sprouting of cortical neurons in Alzheimer's disease. Brain Res 1988;459:138–44
28. Yamazaki M, Arai Y, Baba M, et al. Alpha-synuclein inclusions in amygdala in the brains of patients with the parkinsonism–dementia complex of Guam. J Neuropathol Exp Neurol 2000;59:585–91
29. Goedert M, Spillantini MG, Cairns NJ, Crowther RA. Tau proteins of Alzheimer paired helical filaments: Abnormal phosphorylation of all six brain isoforms. Neuron 1992;8:159–68
30. Umeda Y, Taniguchi S, Arima K, et al. Alterations in human tau transcripts correlate with those of neurofilament in sporadic tauopathies. Neurosci Lett 2004;359:151–54
31. Chin SS-M, Goldman JE. Glial inclusions in CNS degenerative diseases. J Neuropathol Exp Neurol 1996;55:499–508
32. Feany MB, Mattiace LA, Dickson DW. Neuropathologic overlap of progressive supranuclear palsy, Pick's disease and corticobasal degeneration. J Neuropathol Exp Neurol 1996;55:53–67
33. Komori T. Tau-positive glial inclusions in progressive supranuclear palsy, corticobasal degeneration and Pick's disease. Brain Pathol 1999;9:663–79
34. Ikeda K, Akiyama H, Arai T, Nishimura T. Glial tau pathology in neurodegenerative diseases: Their nature and comparison with neuronal tangles. Neurobiol Aging 1998;19:S85–91
35. Wakabayashi K, Oyanagi K, Makifuchi T, et al. Corticobasal degeneration: Etiopathological significance of the cytoskeletal alterations. Acta Neuropathol (Berl) 1994;87:545–53
36. Feany MB, Dickson DW. Widespread cytoskeletal pathology characterizes corticobasal degeneration. Am J Pathol 1995;146:1388–96
37. Tolnay M, Clavaguera F. Argyrophilic grain disease: A late-onset dementia with distinctive features among tauopathies. Neuropathology 2004;24:269–83
38. Powers JM, Byrne NP, Ito M, et al. A novel leukoencephalopathy associated with tau deposits primarily in white matter glia. Acta Neuropathol (Berl) 2003;106:181–87
39. Buee-Scherrer V, Buee L, Hof PR, Leveugle B, et al. Neurofibrillary degeneration in amyotrophic lateral sclerosis/parkinsonism–dementia complex of Guam. Immunochemical characterization of tau proteins. Am J Pathol 1995;146:924–32
40. Goedert M, Spillantini MG, Cairns NJ, Crowther RA. Tau protein of Alzheimer paired helical filaments: Abnormal phosphorylation of all six brain isoforms. Neuron 1992;8:159–68
41. Kuzuhara S, Kokubo Y, Sasaki R, et al. Familial amyotrophic lateral sclerosis and parkinsonism–dementia complex of the Kii Peninsula of Japan: Clinical and neuropathological study and tau analysis. Ann Neurol 2001;49:501–11
42. Mawal-Dewan M, Schmidt ML, Balin B, et al. Identification of phosphorylation sites in PHF-TAU from patients with Guam amyotrophic lateral sclerosis/parkinsonism–dementia complex. J Neuropathol Exp Neurol 1996;55:1051–59
43. Trojanowski JQ, Ishihara T, Higuchi M, et al. Amyotrophic lateral sclerosis/parkinsonism dementia complex: Transgenic mice provide insights into mechanisms underlying a common tauopathy in an ethnic minority on Guam. Exp Neurol 2002;176:1–11
44. Forman MS, Schmidt ML, Kasturi S, et al. Tau and alpha-synuclein pathology in amygdala of parkinsonism–dementia complex patients of Guam. Am J Pathol 2002;160:1725–31
45. Schmidt ML, Zhukareva V, Perl DP, et al. Spinal cord neurofibrillary pathology in Alzheimer disease and Guam parkinsonism–dementia complex. J Neuropathol Exp Neurol 2001;60:1075–86
46. Schmidt ML, Garruto R, Chen J, et al. Tau epitopes in spinal cord neurofibrillary lesions in Chamorros of Guam. Neuroreport 2000;11:3427–30
47. Pérez-Tur J, Buée L, Morris HR, et al. Neurodegenerative diseases of Guam: Analysis of *TAU*. Neurology 1999;53:411–13
48. Zhukareva V, Mann D, Pickering-Brown S, et al. Sporadic Pick's disease: A tauopathy characterized by a spectrum of pathological tau isoforms in gray and white matter. Ann Neurol 2002;51:730–39
49. Zhukareva V, Shah K, Uryu K, et al. Biochemical analysis of tau proteins in argyrophilic grain disease, Alzheimer's disease, and Pick's disease: A comparative study. Am J Pathol 2002;161:1135–41
50. Hogg M, Grujic ZM, Baker M, et al. The L266V tau mutation is associated with frontotemporal dementia and Pick-like 3R and 4R tauopathy. Acta Neuropathol (Berl) 2003;106:323–36
51. Ferrer I, Hernandez I, Boada M, et al. Primary progressive aphasia as the initial manifestation of corticobasal degeneration and unusual tauopathies. Acta Neuropathol (Berl) 2003;106:419–35

ELSEVIER

Journal of the Neurological Sciences 236 (2005) 91 – 93

Journal of the Neurological Sciences

www.elsevier.com/locate/jns

Short communication

Retrograde degeneration of the corticospinal tract associated with pontine infarction

Shunsuke Kobayashi [a,*], Seiji Hasegawa [b], Toshiyuki Maki [c], Shigeo Murayama [d]

[a]*Department of Neurology, Division of Neuroscience, Graduate School of Medicine, University of Tokyo, 7-3-1 Hongo, Bunkyo-ku, Tokyo 113-8655, Japan*
[b]*Hiari Clinic, 1947-10, Hiari, Ohara-machi, Isumi-gun, Chiba 298-002, Japan*
[c]*Maki Clinic, 131 Nishiemi, Kamogawa-shi, Chiba 299-2841, Japan*
[d]*Department of Neuropathology, Tokyo Metropolitan Institute of Gerontology, 35-2, Sakai-cho, Itabashi-ku, Tokyo 173-0015, Japan*

Received 7 February 2005; received in revised form 22 April 2005; accepted 25 April 2005
Available online 29 June 2005

Abstract

We report a 40-year-old man with myotonic dystrophy who survived for 5 years after pontine infarction. Serial MRI detected abnormal T2 elongation of the corticospinal tract at the cerebral peduncle 4 years after the infarction. An autopsy confirmed the existence of retrograde degeneration extending from the pons to the internal capsule, evidence that retrograde degeneration in the corticospinal tract occurs above the pontine level. MRI was suggested to be useful for detection of the degenerative process.

Keywords: Retrograde degeneration; Pyramidal tract; Brainstem; MRI; Myotonic dystrophy

1. Introduction

Retrograde degeneration of the corticospinal tract (RD-CST) of the human central nervous system is considered controversial and exceptional [1–4]. Of the few cases reported, all were secondary to a lesion in the spinal cord. So rare and inconsistent is this phenomenon, even in experimental settings, that the histological characteristics and pathogenesis of RD-CST remain obscure. This is the first report of a case of RD-CST secondary to a brainstem lesion. It was detected by MRI and confirmed by postmortem examination.

2. Case report

A 40-year-old man suddenly developed left hemiparesis and was admitted to our hospital. On arrival CT detected a low-density area at the upper pontine basis with right dominance. He had a history of familial progressive muscle weakness from his second decade. Examination showed severe flaccid left hemiparesis and dysarthria. He was bald in front, and his face had the hatchet-like appearance characteristic of myotonic dystrophy. Grip myotonia and percussion myotonia were present. The diagnosis was pontine infarction with a background of myotonic dystrophy (MD). Brain MRI 4 days after admission showed T1 low T2 high signal areas limited to the pontine basis with right dominance. On the fifth hospital day, he developed ventricular tachycardia with subsequent cardiopulmonary arrest. Immediate resuscitation was successful, but he remained under ventilator control mainly because of MD-related respiratory weakness. MRI four and a half years after admission showed T1-low T2-high proton-high intensity areas in the pons that extended along the CST to the right cerebral peduncle and the internal capsule (IC) (Fig. 1A–D). He died of acute pancreatitis and disseminated intravascular coagulation 5 years after admission.

2.1. Postmortem examination

The unfixed brain weighed 1200 g. After fixation, the cerebrum was evaluated by means of routine serial co-

* Corresponding author. Department of Anatomy, University of Cambridge, Downing Street, Cambridge, CB2 3DY, UK. Tel.: +44 1 223 339544; fax: +44 1 223 333786.
E-mail address: skoba-tky@umin.ac.jp (S. Kobayashi).

0022-510X/$ - see front matter © 2005 Elsevier B.V. All rights reserved.
doi:10.1016/j.jns.2005.04.018

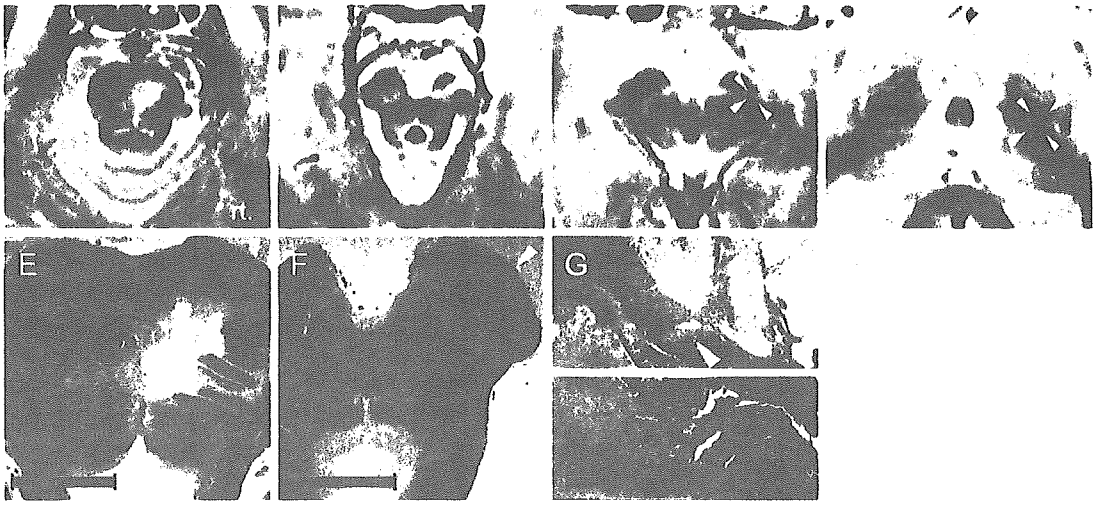

Fig. 1. A–D. Axial slices of magnetic resonance images (TR 3500, TE 19) obtained four and a half years after the patient's pontine infarction. (A) The high intensity area at the pontine base lateralized to the right side corresponds to the original infarction lesion. (B) The high intensity area at the middle part of the right cerebral peduncle shows retrograde degeneration of the corticospinal tract (arrowhead). (C) The high intensity area in the corticospinal tract is smaller and fainter in the upper midbrain slice (arrowheads). (D) The high intensity in the corticospinal tract is traceable rostrally to the internal capsule where it fades out (arrowheads). E–G. Low-power photomicrographs of axial brain sections (Luxol fast blue stain). Scale bar=5 mm. (E) Old cystic infarction at the right upper pontine base. (F) Myelin pallor of poor demarcation at the right middle cerebral peduncle indicates retrograde degeneration of the corticospinal tract (arrowhead). (G) An axial slice in which the posterior limb of the right internal capsule runs beside the globus pallidus. The slit in the middle is due to coronal cutting initially made above the brainstem level. Here, the coronal slices are rearranged in the axial slices to match the MR images taken in the axial direction. Myelin pallor in the corticospinal tract fades out at this level (arrowhead).

ronal sections, and the brainstem and cerebellum by serial axial slices. After routine sampling, the cerebrum was reconstructed, and serial axial sections were compared with axial images of the MRI. An old infarct in the right-side-dominant midline structure of the base of the pons (Fig. 1E) formed a cavity with astrocytic processes and macrophages. There was selective CST loss at the upper pons level, but pontine nucleus and pontine transverse fibers were intact. Midbrain sections showed tissue rarefaction with sparse gliosis in the middle of the cerebral peduncle (Fig. 1F). RD, which could be followed up to the caudal end of the posterior limb of the right IC (Fig. 1G), became obscure at the rostral end. In the cerebral peduncle and IC, large myelinated fibers were markedly lost and small myelinated axons relatively preserved. No astrogliosis or microgliosis were evident. The entire RD length was 30 mm. No significant lesion was detected above the IC level. The orthograde Wallerian degeneration (WD) was traced from the right pons to the caudal end of the examined CST. In the medullary pyramis, both large and small-diameter axons were markedly depleted, and there were prominent isomorphic gliosis and a small number of macrophages. The primary motor area was examined immunocytochemically with anti-gliral fibrillary acidic protein antibody (GFAP, polyclonal, Sigma, Glostrup, Denmark) and HLA-DR antibody (CD68, monoclonal, Nichirei, Tokyo, Japan). No gliosis or neuronophagia was present in the left or right primary motor area.

3. Discussion

Ours is the first report of RD-CST secondary to a brainstem lesion. This case is characterized by a limited lesion at the pontine basis, the only other event being cardiopulmonary arrest 5 days after pontine infarction. Both T2 high intensity on the MRI and myelin pallor on the histological specimen obscured at the level of the IC (Fig. 1D and G). There was no lesion above this level, including in the primary motor cortices. Serial MRI studies at admission and four and a half years after the pontine infarction indicate that CST degeneration developed in the interval between them. These findings indicate retrograde, not orthograde, degeneration starting from the lesion in the pons. Although RD-CST appeared to end in the IC in both the MRI and neuropathological examinations, the end of RD-CST may have been underestimated because CST fibers fan out above the IC which might make detection difficult. The CST location identified as in the posterior limb of the IC is consistent with previous findings including a study that compared MRI and brain specimens from patients with amyotrophic lateral sclerosis [5].

RD or the "dying-back" process that occurs in the peripheral nervous system is caused by a wide variety of toxic, metabolic, and infectious insults [6–8]. The incidence of RD, however, is limited in the central nervous system. To our knowledge, only 12 RD cases in the adult human CST have been reported since 1871 [1–3]. Bronson et al. reviewed 10 of them [2]. Fishman, who examined autopsy

material from 12 patients who had posttraumatic paraplegia, found normal-appearing CST at a distance rostral to the injury [4]. Experimental spinal cord transection in adult mammals has shown that RD-CST begins at the lesion site and slowly advances rostrally over time [9,10].

Brainstem lesions caused by cerebrovascular accidents usually are not restricted to the CST. They often impair vital centers, resulting in a poor prognosis for survival. The shorter survival periods after brainstem lesions as compared with after spinal cord lesions also may be why there is a lower incidence of RD-CST after a brainstem lesion.

It is also possible that MD has something to do with the development of RD-CST [11]. Past reports of RD-CST, however, have not included MD patients. It is more likely that the effect of MD on RD-CST in our patient may have been limited to modification of the disease course after pontine infarction by causing ventricular tachycardia and respiratory weakness.

None of the previously reported RD-CST cases were evaluated by MRI, and RD-CST often was an unexpected autopsy finding. Our report highlights the potential of MRI for detecting RD-CST. Recently, a diffusion tensor imaging technique has been used to detect the structural degeneration of fiber pathways, including WD, after stroke [12]. This technique should prove useful for determining the incidence, development period, speed, and distance of RD-CST.

References

[1] Hunt JR. The retrograde atrophy of the pyramidal tracts. J Nerv Ment Dis 1904;31:504–12.
[2] Bronson R, Gilles FH, Hall J. Traumatic retrograde corticospinal degeneration in man. Hum Pathol 1978;9:602–7.
[3] Yamamoto T, Yamasaki M, Imai T. Retrograde pyramidal tract degeneration in a patient with cervical haematomyelia. J Neurol Neurosurg Psychiatry 1989;52:382–6.
[4] Fishman PS. Retrograde changes in the corticospinal tract of posttraumatic paraplegics. Arch Neurol 1987;44:1082–4.
[5] Yagishita A, Nakano I, Hirano A. Location of the corticospinal tract in the internal capsule at MR imaging. Radiology 1995;194: 289–90.
[6] Schaumburg HH, Wisniewski PS, Spencer PS. Ultrastructural studies of the dying-back process: I. Peripheral nerve terminal and axon degeneration in systemic acrylamide intoxication. J Neuropathol Exp Neurol 1974;33:260–84.
[7] Sima AA, Bouchier M, Christensen H. Axonal atrophy in sensory nerves of the diabetic BB-Wistar rat: a possible early correlate of human diabetic neuropathy. Ann Neurol 1983;13:264–72.
[8] de la Monte SM, Gabuzda DH, Ho DD, Brown Jr RH, Hedley-Whyte ET, Schooley RT, et al. Peripheral neuropathy in the acquired immunodeficiency syndrome. Ann Neurol 1988;23:485–92.
[9] Kalil K, Schneider GE. Retrograde cortical and axonal changes following lesions of the pyramidal tract. Brain Res 1975;89: 15–27.
[10] Pallini R, Fernandez E, Sbriccoli A. Retrograde degeneration of corticospinal axons following transection of the spinal cord in rats. A quantitative study with anterogradely transported horseradish peroxidase. J Neurosurg 1988;68:124–8.
[11] Chen XQ, Tan I, Leung T, Lim L. The myotonic dystrophy kinase-related Cdc42-binding kinase is involved in the regulation of neurite outgrowth in PC12 cells. J Biol Chem 1999;274:19901–5.
[12] Werring DJ, Toosy AT, Clark CA, Parker GJ, Barker GJ, Miller DH, et al. Diffusion tensor imaging can detect and quantify corticospinal tract degeneration after stroke. Neurol Neurosurg Psychiatry 2000;69: 269–72.

Possibility for Neurogenesis in Substantia Nigra of Parkinsonian Brain

Kenji Yoshimi, PhD,[1] Yong-Ri Ren, MD,[2] Tatsunori Seki, PhD,[1,3] Masanori Yamada, PhD,[1] Hideki Ooizumi, MD,[2] Masafumi Onodera, MD, PhD,[4] Yuko Saito, MD, PhD,[5] Shigeo Murayama, MD, PhD,[5] Hideyuki Okano, MD, PhD,[6] Yoshikuni Mizuno, MD, PhD,[1,2] and Hideki Mochizuki, MD, PhD[1,2]

Recent studies of enhanced hippocampal neurogenesis by antidepressants suggest enhancement of neurogenesis is a potentially effective therapy in neurodegenerative diseases. In this study, we evaluated nigral neurogenesis in animals and autopsy brains including patients with Parkinson's disease (PD). First, proliferating cells in substantia nigra were labeled with retroviral transduction of green fluorescent protein, which is an efficient method to label neuronal stem cells. Subsequent differentiation of labeled cells was followed; many transduced cells became microglia, but no differentiation into tyrosine hydroxylase–positive neurons was detected at 4 weeks after injection, in both intact rodents and those treated with 1-methyl-4-phenyl-1,2,3,6-tetrahydropyridine. Second, polysialic acid (PSA)–like immunoreactivity, indicative of newly differentiated neurons, was detected in the substantia nigra of rodent, primate, and human midbrains. A large number of PSA-positive cells were detected in the substantia nigra pars reticulata of some patients with PD. In rats and a macaque monkey, the dopamine-depleted hemispheres showed more PSA staining than the intact side. A small number of tyrosine hydroxylase–positive cells were PSA-positive. Our results suggest enhanced neural reconstruction in PD, which may be important in the design of new therapies against the progression of PD.

Ann Neurol 2005;58:31–40

Neurogenesis in the hippocampus is essential for the therapeutic effect of antidepressants.[1–3] Enhancement of neurogenesis may open a new therapeutic potential in other central nervous system diseases, especially neurodegenerative diseases.[4] The potential of neurogenesis has been reported in Huntington's disease and Alzheimer's disease.[5–7] In Parkinson's disease (PD), the loss of dopaminergic neurons in the substantia nigra (SN) is the major pathological change.[8] Surgical replacement of dopaminergic neurons was reported to be effective in some patients, but the induction of severe uncontrolled off-medication dyskinesia limits its therapeutic usefulness.[9] If intrinsic dopaminergic neurons could be regenerated in SN of patients with PD, the enhancement of such process should be the primary therapeutic target.

The potential of neurogenesis in the SN has been studied by labeling proliferative neural precursor cells with bromodeoxyuridine (BrdU).[10–13] Because a compensatory enhancement of neurogenesis in the hippocampus has been reported after brain injury,[14–16] the brains have been examined for neurogenesis after dopaminergic cell deprivation, as well as in the intact brains. Kay and Blum[10] report the presence of BrdU-positive proliferative cells in the SN; a part of such cells were microglia, but none of them differentiated into dopaminergic neurons. In another study,[11] neuronal progenitor cells isolated from the SN of rats differentiated to neurons in the hippocampus but not in the midbrain. Using confocal laser scanning microscope, Zhao and colleagues found dopaminergic neurons with BrdU-positive nuclei in the SN, which were considered to have migrated from the midbrain aqueduct,[12] although a different conclusion was reported in another study.[13] The discrepancy between the two studies[12,13] was due to the uncertainty of whether BrdU-positive nuclei were located in or out of the tyrosine hydroxylase (TH)–positive cytoplasm. Another problem was that at a high dose, BrdU could be incorporated into repairing, as well as duplicating, DNA.[17,18]

From the [1]Research Institute for Diseases of Old Ages, Juntendo University; Departments of [2]Neurology and [3]Anatomy, Juntendo University School of Medicine, Bunkyo-ku, Tokyo; [4]Department of Hematology, Institute of Clinical Medicine, University of Tsukuba, Tsukuba, Ibaraki; [5]Department of Neuropathology, Tokyo Metropolitan Institute of Gerontology, Itabashi-ku; and [6]Department of Physiology, Keio University School of Medicine, Shinjuku, Tokyo, Japan.

Received Jan 18, 2005, and in revised form Apr 4. Accepted for publication Apr 5, 2005.

Published online May 23, 2005, in Wiley InterScience (www.interscience.wiley.com). DOI: 10.1002/ana.20506

Address correspondence to Dr Mochizuki, Department of Neurology, Juntendo University School of Medicine, 2-1-1 Hongo, Bunkyo-ku, Tokyo 113-8421, Japan.
E-mail: hideki@med.juntendo.ac.jp

Published by Wiley-Liss, Inc., through Wiley Subscription Services

BrdU is not the only tool to label DNA synthesis in proliferating cells. Retroviral labeling is another method, which has several advantages to BrdU labeling.[19,20] Specific marker genes can be transducted into duplicating chromosomes by retroviral vectors. The expression requires following protein synthesis; thus, the expression of green fluorescent protein (GFP) is highly specific to the cells that proliferate at the time of infection. We efficiently labeled neuronal stem cells with GFP by retroviral transduction, both in vitro and in vivo.[21–23] In these studies, GFP filled the cytoplasm of the cells and expressed a clear Golgi-like morphology of the infected cells. Moreover, local injection in the brain tissue allowed a clear mapping of the migration route.[19,22]

Labeling of proliferating cells with BrdU and retrovirus may not be the only methods to detect neurogenesis. Intrinsic molecules unique to young neurons, such as polysialic acid (PSA) and doublecortin, can be used as tools to detect neurogenesis.[24,25] This is especially important in human subjects, where experimental markers such as BrdU or retroviral vectors are not applicable.

In the first part of this study, we observed the fate of endogenous proliferating cells in rodent SN by examining the morphology of cells after retroviral transduction of GFP. Retroviral injection close to the midbrain aqueduct also was performed to confirm the possible migration of cells derived from neural stem/progenitor cells from this area to the SN. In the second part of this study, we analyzed immunostaining of PSA in human SN tissues of patients with PD and dopamine-deficit animals.

Materials and Methods

Animals and Drug Administration

Adult C57BL/6 mice (10-week-old female) and Sprague–Dawley rats (10-week-old male) were obtained from Charles River Laboratories (Yokohama, Japan). They were housed two to six per cage and maintained on a 12-hour light–dark cycle at constant temperature and humidity. Food and water were provided ad libitum. The animals injected with retrovirus vector (see later) were kept in air-isolated cages with Hepa filter ventilation system. The experimental protocol was approved by the Ethics Review Committee for Animal Experimentation of Juntendo University School of Medicine. Mice were injected with 1-methyl-4-phenyl-1,2,3,6-tetrahydropyridine (MPTP; Sigma Labs, St. Louis, MO) or saline in acute (20mg/kg body weight intraperitoneally (IP) four times a day at 2-hour intervals) or chronic (30mg/kg once a day for 5 days) protocols(Table 1).[26] MPTP was handled carefully, and the remaining solutions were inactivated with bleach.[27]

Preparation of Modified Retroviral Vector

The retroviral vector GCDN sap carrying enhanced GFP gene was packaged with vesicular stomatitis virus G protein (VSV-G) by transduction into 293gpg as described previously.[20–22] The virus producer clone (293gpg/DNEGFP) was harvested in Dulbecco's modified eagle medium with 10% fetal bovine serum (FBS) and tetracycline. When 10 flasks (900ml) became 70% confluent, tetracycline was removed to start the production of the virus under the control of tet-off system. Two days later, the medium was centrifuged at 6,000× *g* and 4°C, followed by resuspension of the viral pellet in phosphate-buffered saline (PBS). Finally, the viral vector was centrifuged to 1,000-fold concentration and stored at −80°C. All containers and tools used to handle retroviral vectors were rinsed with ethanol or disposed after autoclaving.

Stereotaxic Injection of Retroviral Vector

Concentrated viral solution was injected into the mouse SN bilaterally, 1μl into each side. Mice were anesthetized with pentobarbital (60mg/kg body weight IP), then held on a stereotaxic frame, drilled on the skull, and a 31-gauge needle was inserted into the SN (anteroposterior [AP], −2.8 mm; mediolateral [ML], 1.3mm from bregma; dorsoventral [DV],

Table 1. MPTP Administration Schedule for Retroviral Labeling in Mice and Rats

	Target	MPTP	Days to surgery	Survival	Group	n
Mice	Nigra	Sal × 4	2	4 weeks	Sal2d4w	7
		20 × 4	2	4 weeks	A2d4w	8
		20 × 4	7	4 weeks	A7d4w	6
		30/d × 5d	7	4 weeks	C7d4w	4
		Sal × 4	2	16 weeks	Sal2d16w	4
		20 × 4	2	16 weeks	A2d16w	4
	Aqueduct	Sal × 4	7	4 weeks	Sal7dAq4w	3
		20 × 4	7	4 weeks	A7dAq4w	6
Rats	Nigra			2 days	R-SN2d	5
				2 weeks	R-SN2w	3
	Aqueduct			2 days	R-Aq2d	2
				2 weeks	R-Aq2w	6
				4 weeks	R-Aq4w	7

MPTP = 1-methyl-4-phenyl-1,2,3,6-tetrahydropyridine.